Edge-Lit Holographic Stereograms

by

William John Farmer

B.A., Mathematics
College of the Holy Cross
Worcester, Massachusetts
1971

Submitted to the Media Arts and Sciences Section,
School of Architecture and Planning
in partial fulfillment of the requirements
for the degree of

Master of Science

at the

Massachusetts Institute of Technology

June 1991

Signature of Author _____
Media Arts and Sciences Section
May 10, 1991

Certified by _____
Stephen A. Benton
Professor of Media Technology
Thesis Supervisor

Accepted by _____
Stephen A. Benton
Chairman
Departmental Committee on Graduate Students

Edge-Lit Holographic Stereograms

by

William J. Farmer

Submitted to the Media Arts and Sciences Section,
School of Architecture and Planning, on May 10, 1991
in partial fulfillment of the requirements of the degree of
Master of Science at the Massachusetts Institute of Technology

Abstract

The edge-lit hologram display format has been successfully extended to holographic stereograms. Taking advantage of the discrete nature of the information content of stereograms, the three step production process of edge-lit rainbow holograms has been reduced to a two-step process for edge-lit holographic stereography. Design improvements have been made to the edge-lit's immersion recording tank. The image distortion resulting from refraction as the object beam transits the air-tank interface in the final recording stage has been investigated and compensation techniques developed.

Thesis Supervisor: Stephen A. Benton
Title: Professor of Media Technology

This research was supported in part by the Hughes Aircraft Company, as part of their sponsored research program at the Media Laboratory under contract number 7-N73323R9JE, and by the Design Staff of the General Motors Corporation.

Dedication

This thesis is dedicated to two men by way of thanks. It is apparent to me that without their support I wouldn't now be here completing this.

To: Russell K. Hobbie
Associate Dean of the Institute of Technology
University of Minnesota, Minneapolis

for having put a human face on a vast bureaucracy.

and

To: Steven K. Case
Professor of Electrical Engineering
University of Minnesota, Minneapolis

for giving his time when he really didn't have any to give.

Acknowledgements

First and foremost, I would like to thank Stephen Benton for accepting me into his group, for providing a work space that would be the envy of most holographers, and for his advice and guidance.

To my fellow members of the Spatial Imaging Group, I thank you for your comradarie and for your various help, too great to elaborate. Don't think your getting rid of me either. I'll be there to dance on all your graves.

To all the support staff, Linda, Lena, et al., thank you for your help, thank you for your forbearance.

Thanks to my family, Aunt Al, LI, MN, and CA for their important support, financial and emotional.

To my friends in Minnesota, who let me take "time-out", for a couple of years. About ready to call "time-in".

Ken, you've made me laugh even when I wanted to be angry. Write when you find work.

Saving the profoundly heartfelt til last, to my dear and beautiful wife, Yuriko. I don't know the words in either language that can do justice to my feelings of gratitude and love. Thank you for your patience and support, for allowing me to get as much as I could from the MIT experience. You're one in a million. I love you.

Contents

List of Figures

Chapter 1

Background

1.1 Introduction

The proliferation of holographic images into a broad new range of display venues hinges on the dual requisites of producing stunning images that can be effortlessly displayed. The research reported in this thesis set out to unite two disparate lines of research, each uniquely satisfying one of the two requisites. Holographic stereography, empowered by the computer, has become a mature medium capable of producing beautiful art holograms and also startlingly realistic visualization of scientific data. On the other hand, the edge-lit display format is a fledgling, newly arrived on the holography scene, but holding the promise of eliminating the cumbersome impediments inherent in mounting a holographic display.

Research towards this thesis began with the redesign and engineering of an important piece of equipment used in edge-lit recording, the immersion exposure tank. Although this was the first aspect of research, it is not reported until the end

of this thesis (Chapter 5), being outside the central thrust of the research.

The central thrust is the extension of the edge-lit display format to holographic stereograms. The stereogram, because of the discrete nature of its constituent perspective images, is a gracious and malleable medium. The ability to utilize a computer to manipulate the perspective images of a stereogram renders it generally compliant to experimentation. Such was the hope going in, such is the result coming out. Because of this predisposition of the stereogram to flexibility, we were able, in this research, to realize a simplification of the edge-lit recording process, eliminating one recording step to reach a two-step process. Chapter 2 will demonstrate the concordant relationship between stereography and computer manipulation, by detailing the specifics of how the simplification of the recording process was achieved.

Because edge-lit production employs refractive-index matched immersion recording in the transfer stage, the information bearing image wave passes through a refractive interface. The effect of this refraction on our edge-lit stereogram's final image was severe distortion. In Chapter 3, we report and quantify our success in developing a compensation technique to assuage the effect of refraction. This technique has been experimentally tested, resulting in the production of visually satisfying edge-lit stereograms.

Yet some small imperfections remained in the final image after the application of this compensation technique. In Chapter 4, we posit a second compensation technique that, in principle, corrects one of the two small remaining defects. This second technique has yet to be put to the experimental test.

The remainder of this chapter will set the table by briefly reviewing the historical developments of the holographic stereogram and the edge-lit display format,

1.2 Holography and Holographic Stereography

The phenomenon of holography, the 1948 discovery[1] of which earned a Nobel Prize for Dennis Gabor, proved prohibitively challenging until buoyed by the invention of the laser. Thereafter, concurrent with research and advances in optical holography itself, investigation was undertaken into possible application of holography to other formats. Because of the extreme stability requirements of holographic recording—movement on the order of a hundred nanometers of the recording apparatus during exposure will likely destroy the information—subject matter that is suitable for holography is greatly restricted; holography is essentially restricted to "small dead things". Notably, organic matter is recorded only with great difficulty. Application research was successful in providing a format in which the range of suitable subject matter was greatly, in fact infinitely, extended. This application research, which will be noted below leads directly to the current holographic stereogram.

A hologram is an analog information carrier. Perspective information varies continuously across the spatial extent of the hologram. Using holographic techniques to overcome limitations of a recording technique proposed by Lippmann[1] at the turn of the century, McCrickerd and George in 1968[2] recorded a dense two-dimensional array of perspective views, thereby creating in effect a discretized version of a hologram. Consideration of the psychophysics of human sight led to the reduction of the discrete hologram to a horizontal-parallax-only version, greatly reducing the nonessential and redundant information content of the discrete hologram. This version of the discrete hologram emerged from the work of DeBitetto[3, 4] and represents the seminal holographic stereogram.

In holographic stereogram production, a continuous series of perspective views

[1]Lippmann proposed that a fly's eye lens, an array of small spherical lenses, could record various perspectives on a single emulsion from which an image with parallax could be projected

are recorded on ciné film. The subject matter can be anything that can be filmed. In the modern world, this is no longer limited to what is visible to the naked eye. With the emergence of computer rendering sophistication, anything for which three-dimensional spatial data can be collected, as well as any image that can be imagined and rendered is a candidate for holographic stereogram recording. Each of the sequential two-dimensional views is subsequently recorded as a very narrow (generally 1–3 mm wide) hologram. These narrow holograms are aligned sequentially on a single recording plate, and in the same sense that mathematical integration can be modeled by the summation of a continuum of areas of minimal width, so too do these narrow perspective recordings essentially integrate into a horizontal-parallax-only hologram.

A major line of research in holographic stereograms (hereafter referred to simply as stereograms) aimed at and succeeded in white light viewability. A two step transfer process which emerged from Bell Labs[5] resulted in achromatic or black-and-white images when illuminated by white light. With images of depths of more than a few centimeters, however, problematic color smearing resulted. A refined technique developed by Benton[6] took into account the relative positions of the various spectral components of the playback image by introducing an angular relationship, the so-called achromatic angle, between the master and the transfer plates. This enabled the production of achromatic images of considerable depth. Moreover, by multiplexing more than one master onto a transfer plate, multi-color stereograms could be created.

Another approach to color stereograms originated with the work of Denisyuk[7] whose work focused on Bragg wavelength selection in thick reflection holograms. Hariharan[8] employed emulsion swelling between multiple exposures to create holograms which selected more than one wavelength, thus creating multi-color reflection holograms. This so-called pseudocolor technique has been vastly improved by research at the Media Lab[9] resulting in beautiful full-color reflection stereograms.

1.3 Stereography Research at the Media Lab

Because of its superiority as a three-dimensional display medium, the holographic stereogram has been the focus of much research in the Spatial Imaging Group of the Media Lab. In its brief history, the lab has contributed significantly to the improvement of stereograms, leading the way in elevating the current state of the art. The contributions of the Spatial Imaging Group have included research in new geometrical configurations for stereograms[10, 11], computer manipulation of image data to compensate for optical recording distortion[12], creation of a facile RGB color mixing technique for reflection stereograms[9], and scaling up the size of the stereogram[13].

Most recently, research has led to a technique that, by using computer predistortion of images, allows for a broad range of new recording and viewing configurations[14, 15]. An equally broad range of benefits has been realized from this technique, such as opening the view angle of the final image of stereograms from approximately 30° to over 100°. This technique plays a significant role in the success of the research reported here, and will be described in some detail in Chapter 2.

The application of these advances has resulted in the recent production of a wide variety of high quality stereograms at the Media Lab, ranging from portraiture, through scientific visualization, to artistic display.

All of these stereograms, however, are displayed with a geometrically specific external illumination source, and changing their display venue is accomplished only with some difficulty.

1.4 The Edge-lit Display Format

The edge-lit display format was developed in the Spatial Imaging Group[16], adapting a strategy from laser-lit head-up display technology[17], and applying it to display holography with white light. This display format does not require the distant external illumination that has held back the infiltration of holograms into a larger array of display venues. Using a broadband illumination source in the base used to support a hologram, the edge-lit format allows the integration of the hologram and its illumination source into a compact unit.

The name "edge-lit" is actually a bit of a misnomer, suggesting that the hologram itself is illuminated through its edge. An earlier, though less glamorous name, "steep reference angle" holography conjures a more accurate image of the what is actually involved optically. In its display format, an edge-lit hologram is laminated to a glass block with a refractive-index matched epoxy. The glass block is on the order of an inch thick. During playback, as diagrammed in Figure 1.1, the edge of the glass block is illuminated at near normal incidence, transmitting, with minimal refraction, nearly vertical rays into the glass. These rays impinge at a very steep angle upon the glass face holding the hologram . These rays are transmitted to the glass substrate of the emulsion and enter the emulsion at angles much steeper than have previously been achievable. In addition to allowing for the placement of the illumination source below and very close to the hologram, this illumination geometry widens the vertical view angle.

The use of a nearby illumination source precludes the use of conjugate illumination. A conjugate scheme would require that the reference beam focus to an equally proximate point while still illuminating the transfer plate in its entirety. This would require very large and expensive optics and is not feasible. Instead, a technique that was developed for achromatic rainbow holograms was adapted and applied[18].

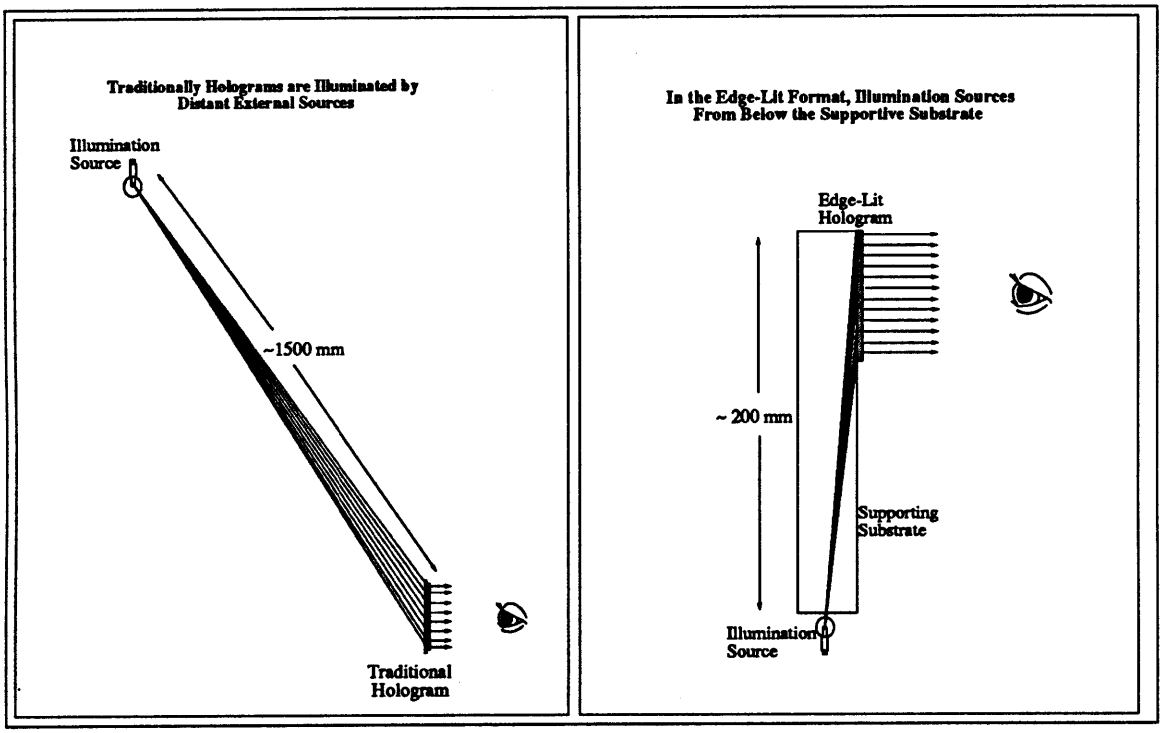

Figure 1.1: The edge-lit display format overcomes the problems inherent in distant, external illumination sourcing characteristic of traditional hologram illumination.

This technique decouples final image reconstruction from the requirement of distant illumination.

According to this technique, in the first transfer, a master's conjugate image is projected downstream beyond the original object plane and recorded in a first transfer. This transfer is played back with conjugate illumination, so that the image wave retraces a path identical to the first transfer stage but with reversed direction. In this second transit, the image is recorded in the object plane using a near-by reference source. This recording, the second transfer, is played back with a broadband illumination source in direct mode, i.e., with a geometrical relation to the hologram identical to the reference source. Because each stage uses either exact conjugate or direct illumination, a distortion-free final image is produced.

Edge-lit holographic recording makes use of this three-step process. The direct illumination used in the edge-lit display is propagated through the base of a substrate that supports the hologram. Correspondingly, in its original methodology, the edge-lit hologram's final transfer was accomplished by index-matching the transfer plate to a supporting substrate and introducing its reference beam through the substrate's base.

Rainbow holograms that were recorded with this original edge-lit technique suffered from image artifacts. These artifacts were caused by spurious gratings resulting from Fresnel reflections at the various refractive-index interfaces in the vicinity of the emulsion[19]. Index-matched immersion recording of the final transfer was proposed as a solution to the problem of spurious gratings; recording the final transfer in an index-matching liquid moved the largest of the index mismatches far from the emulsion. A prototype index-matched immersion tank was designed and constructed for testing the viability of the immersion method[20].

1.5 Conclusion

Though the holographic stereogram has a rich history, and has developed to a point where rich and vivid images are the norm, the difficulties inherent in holographic display impede the ascendance of holography to a more prominent role in the realm of display media. The easing of the problems of display would open new venues to holographic display. The early results of the edge-lit display research raised the hope that it might provide a technique and a display format that would overcome these problems.

Overcoming the display obstacles will not be completely achieved by extending the edge-lit format to stereograms. This extension will only be a gross first step. There will remain the detailed work of extending the myriad of experimental advances of stereography to the edge-lit but applying each technique in a way that accommodates for the idiosyncrasies of the edge-lit's recording technique and display. It was with the hope of achieving this first step that the research reported in this thesis was undertaken.

In the next chapter, we will describe how a new type of holographic stereogram has made the integration of stereography and the edge-lit display congruous.

Chapter 2

The Role of the Ultragram

2.1 Background

The viewing system of multi-step white-light-viewable holograms and stereograms is such that one observes the image by looking through an exit pupil or viewing window that is the projected image of the master hologram. This is normally accomplished by playing back the transfer hologram with near-conjugate illumination. As cited earlier, the edge-lit technique has employed a three-step recording process that enables the exit pupil to be played out with direct illumination.

In stereogram viewing, the exit pupil is the projected image of the master and is, therefore, composed of the projected images of the slit holograms that make up the master. When the viewer places his or her two eyes into the projected image of two distinct slits, the viewer observes a stereo-pair of perspective views and stereopsis is satisfied. The reduction of the production process of edge-lit stereograms to two-steps was made possible by the recent work of Halle, who has developed a stereogram

recording geometry, called the "Ultragram", that relaxes these historical viewing constraints[14, 15].

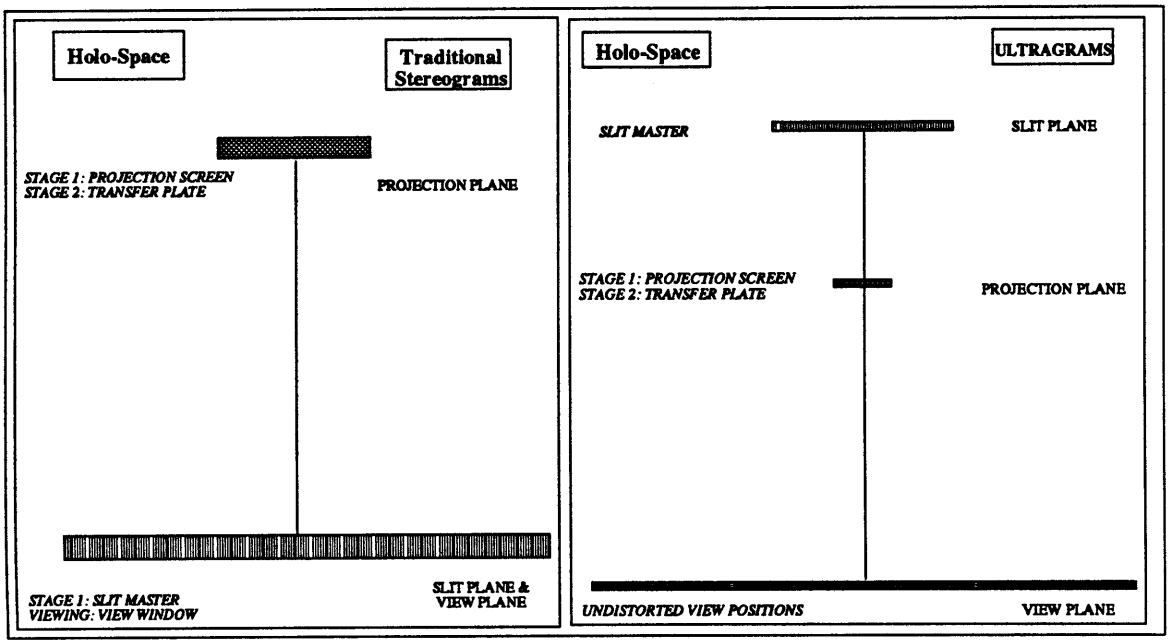

Figure 2.1: The Ultragram technique allows separation of the Slit Plane and the View Plane, relaxing traditional viewing constraints.

The Ultragram system uses computer predistortion of the discretely recorded images to permit a shuffling of the three constituent planes of stereogram space. Figure 2.1 shows a comparison of the geometry of traditional stereogram viewing to Halle's Ultragram geometry that was used in production of the edge-lit stereogram. With a geometry in which the Projection Plane lies between the Slit Plane and the View Plane, direct (as opposed to conjugate) illumination can be used to play out the virtual (as opposed to real) image of the slit master. Predistortion of the images of the slit master exactly compensates for the image distortions this geometry introduces. Freed from the geometrical constraint of having Slit Plane and View Planes coincide, direct illumination can be used for the playback of the edge-lit stereogram transfer

without the extra transfer step required in edge-lit rainbow holography.

2.2 The Ultragram

The traditional stereogram has a single recording configuration and as a result a single viewing scheme. In recording, integral perspective views of a scene are sequentially recorded in the master as slit holograms. These slit holograms are simultaneously multiplexed in a transfer hologram by recording the conjugate image projected from the master hologram. When the conjugate image of this transfer hologram is projected, the image content of the stereogram is viewable through a viewing window. This viewing window is the image of the master hologram, and the space of the viewing window is segmented into the slit pattern that partitioned the master hologram. The image content of each of these slit segments is a perspective view of the scene appropriate to its position in the composition of the master.

The viewing structure is like a picket fence. Imagine a young fan viewing a baseball game through such a picket fence. By putting each of his eyes in a space between the pickets, he is able to view the event without impediment. As diagrammed in Figure 2.2, the metaphorical pickets in the view window of the traditional stereogram are the points of transition from one slit to the next. The space between pickets is the area of the slit, and this space is filled with the perspective image appropriate to that slit. Because the image content of each slit is an integral perspective view, the only viewing geometry possible is one in which the Slit Plane coincides with the View Plane.

The viewing limitation of the traditional stereogram results from the fact the the image stored in each slit needs to be an integral two-dimensional view of the scene being recorded. With advancements in computer-based technology and the

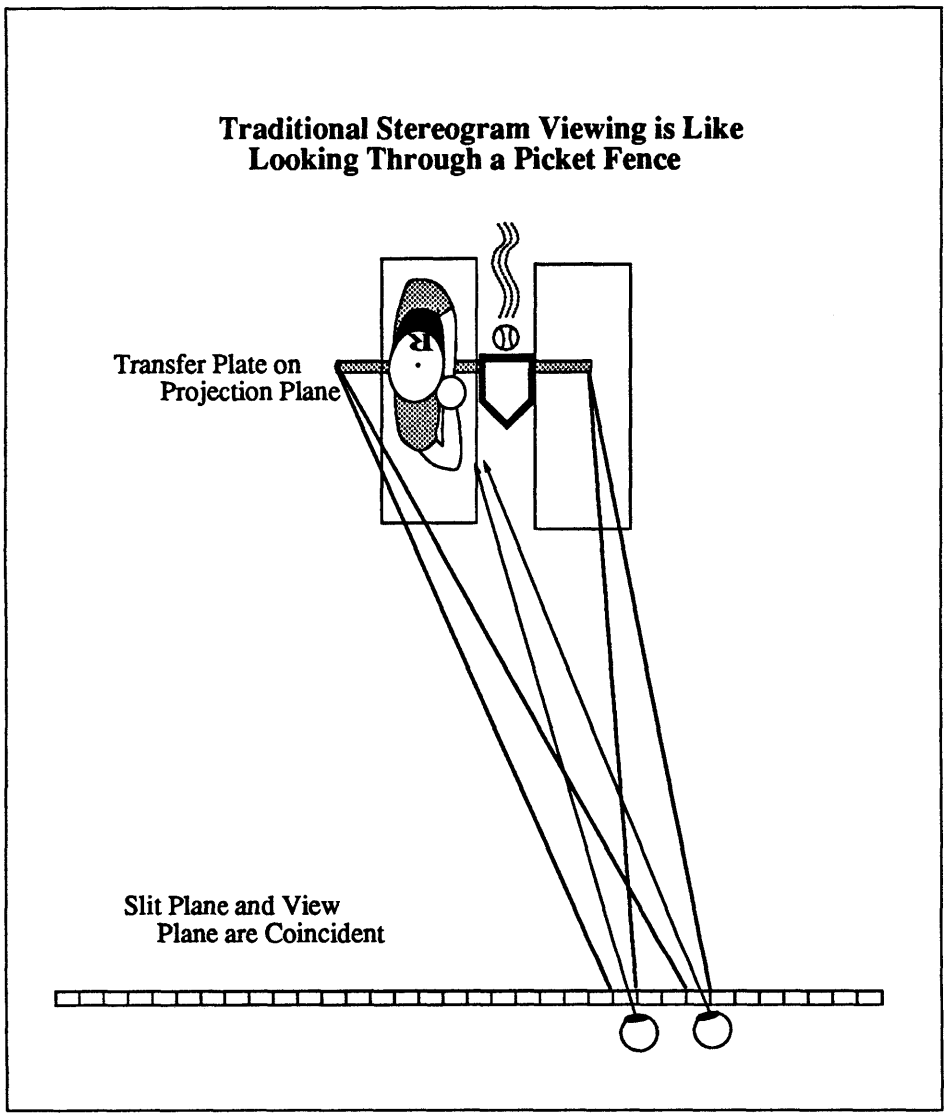

Figure 2.2: Viewing a traditional stereogram, the viewer puts each eye in the projection of a different slit. The slit projection is filled with the projected image appropriate to the slit's view perspective.

digitizing of images, it was possible to use computer manipulation of the images to break through this limitation. The key to overcoming the limitation was to be able to separate the View Plane from the Slit Plane, an alteration that required a single perspective view to be shared amongst several slits. To see this, let's go back to our young baseball fan. If he stands, not along the picket fence, but rather some distance removed from the the fence, as shown in Figure 2.3(a), his view of the game arrives through multiple slits. The Ultragram viewing system synthesizes a similar construct by carefully matching slits and portions of the image projected on the Projection Plane for each viewposition along the View Plane. As shown in Figure 2.3(a), the image delivered to a specific viewposition is a composite of slices of the projection screen, with each slice passing through a different slit. Equivalently, as shown in Figure 2.3(b), each slit will contribute a different slice of the Projection Plane to a large number of discrete viewpositions. To bring this about, the image recorded in a slit must be a composite of slices from various perspective views. This matching of viewposition to slit and image slice is the hallmark of the Ultragram system. New images, composited from the individual slices that pass through the same slit, are fabricated by a technique dubbed "slice-and-dice", and the composited images are those that are recorded in the master.

Having separated the Slit Plane from the View Plane, and established the procedure of compositing new images to be recorded in the slits, it becomes possible to shuffle the three planes of the Ultragram space to arrive at new configurations which expand the stereogram taxonomy and the holographer's repertoire. If we geometrically shuffle the positions of the Slit Plane and the Projection Plane, as shown in Figure 2.4 we arrive at a valuable result. As can be seen, the "slice-and-dice" procedure is applicable to this configuration as well. During the mastering stage, the image propagates from the Projection Plane to the Slit Plane. When playing out a holographic recording, conjugate illumination can be used to send the image back in

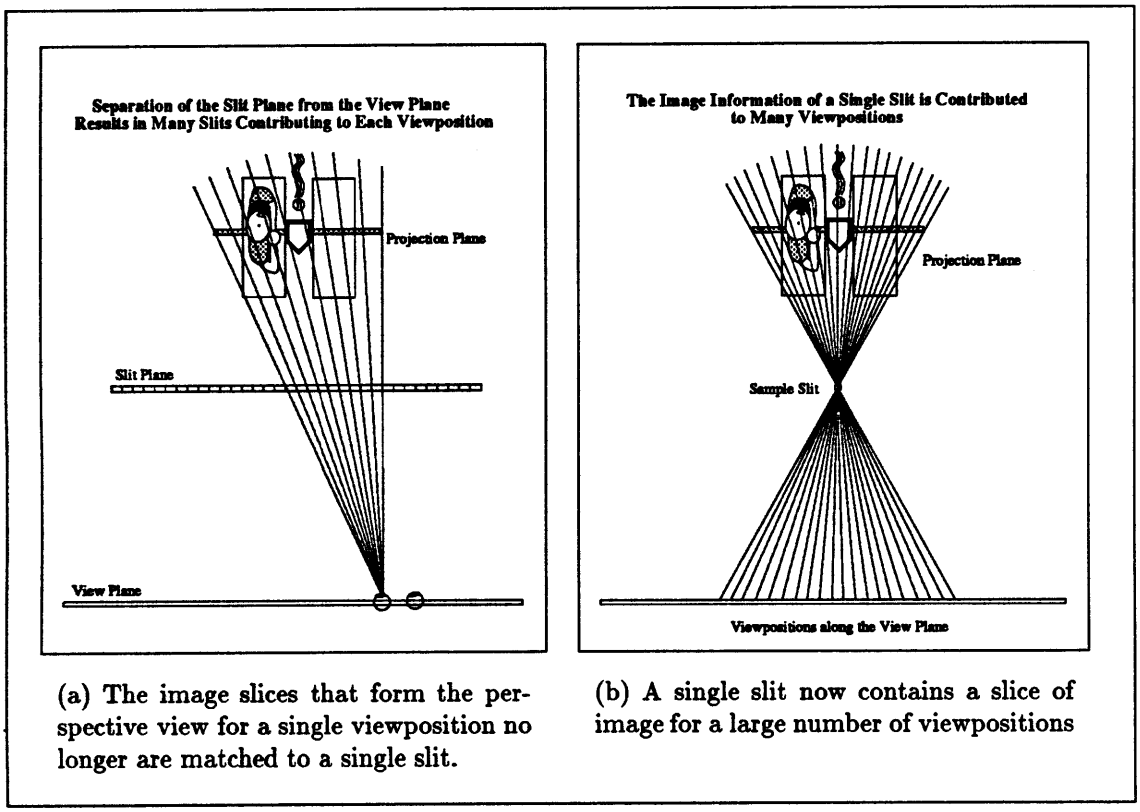

(a) The image slices that form the perspective view for a single viewposition no longer are matched to a single slit.

(b) A single slit now contains a slice of image for a large number of viewpositions

Figure 2.3: Separating the View Plane from the Slit Plane destroys the one to one pairing of slit and viewposition.

the direction whence it came, or direct illumination can be used to continue it in the direction in which it was traveling during recording. During the transfer stage, the image returns from the Slit Plane to the Projection Plane, which is now occupied by the transfer plate. Conjugate illumination is used in this stage to cause the image to retrace its path. But, during reconstruction, with the new configuration diagrammed in Figure 2.4, the image will propagate to the View Plane by traveling in the same direction it traveled during the transfer stage. Therefore, direct illumination will be used. Because the edge-lit technique requires direct illumination of the final image, this Ultragram configuration is ideally suited to the edge-lit display. Using this Ultragram configuration, an edge-lit stereogram can be produced in two steps, a saving of one step over the three steps required with edge-lit rainbow holography.

2.3 Production Steps

The edge-lit stereogram described here was produced with a two-step process, diagrammed in Figure 2.5. The 300 mm x 300 mm slit master contained three hundred 1 mm holographic recordings of predistorted images. In recording, these images had been rear projected onto a 100 mm x 100 mm diffusing screen, set parallel to the slit master recording plate and separated from it by 250 mm. The final view distance is used in the algorithms to calculate and execute the predistortion and must be prescribed by the holographer. In our case, a view distance of 500 mm was selected. Aside from the predistortion of the images, the only other variance from standard stereogram-master recording procedure was the fact that the master recording plate and the projection screen remained geometrically fixed with respect to one another, while the 1 mm slit moved relative to both.

In the transfer stage, the image of the slit master was projected by conjugate

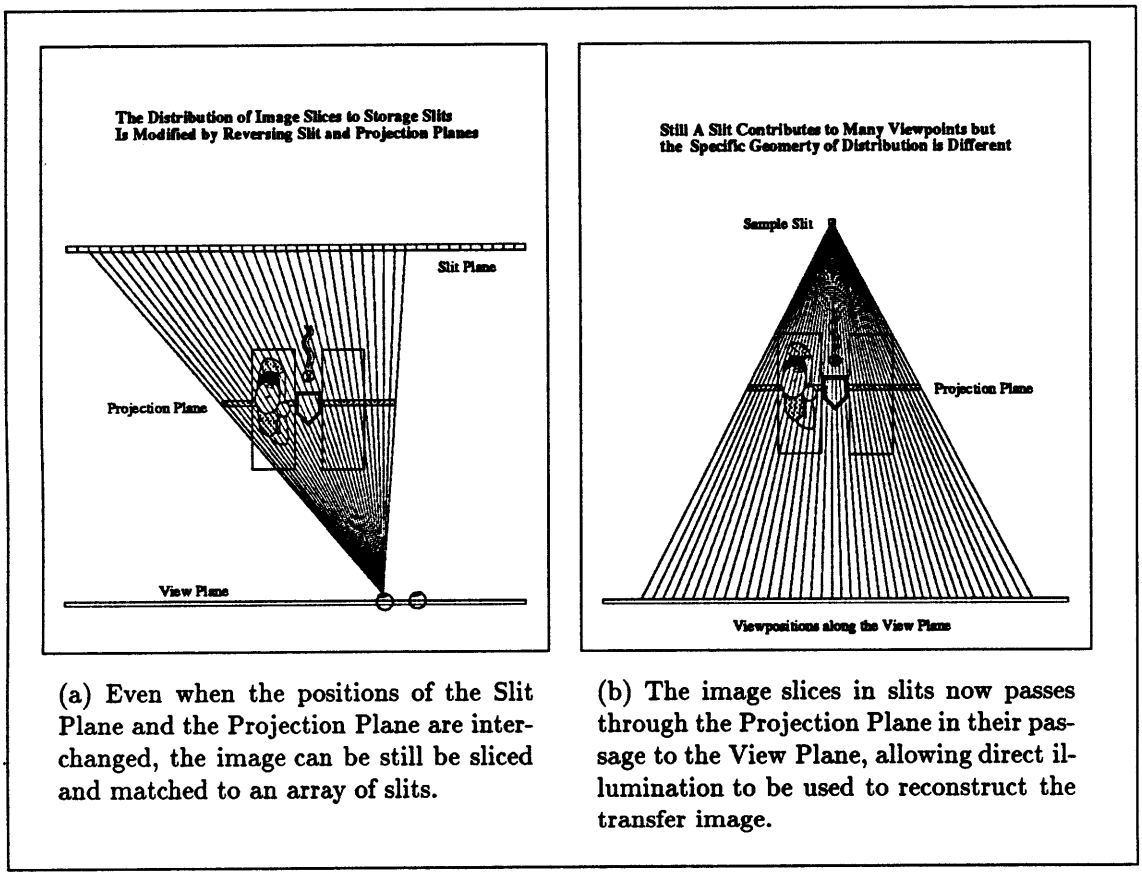

(a) Even when the positions of the Slit Plane and the Projection Plane are interchanged, the image can be still be sliced and matched to an array of slits.

(b) The image slices in slits now passes through the Projection Plane in their passage to the View Plane, allowing direct illumination to be used to reconstruct the transfer image.

Figure 2.4: A configuration of Ultragram space that interchanges the positions of the Slit and Projection Planes, creates a recording geometry ideally suited to the needs of the edge-lit display.

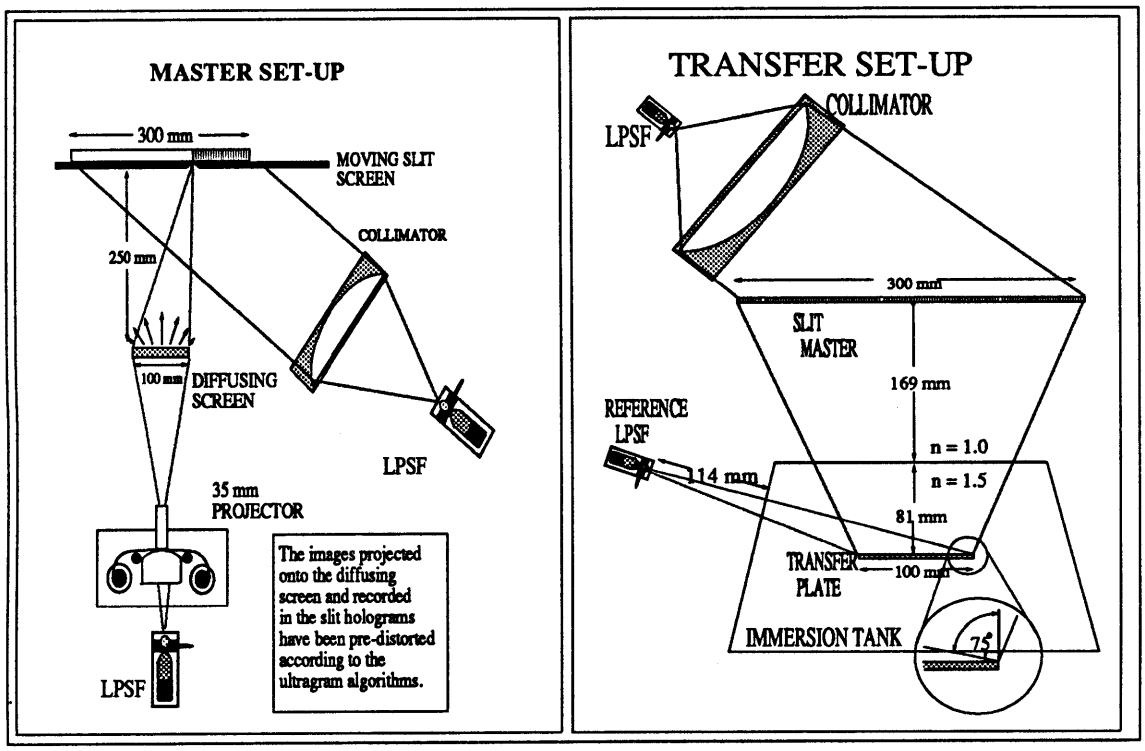

Figure 2.5: The The two-step edge-lit stereogram production technique relies on computer predistortion of the images recorded in the master, and the use of immersion recording for the transfer.

illumination, transitted the front window of the exposure tank, propagated through the index matching liquid, and fell upon the transfer recording plate. There, it interfered with a reference beam that diverged from a coherent point source outside the side wall of the tank.

Playback with direct illumination should, in principle, result in an undistorted final image.

2.4 Consideration of Halle's Geometry to Determine View Parameters

Using Halle's geometry, we can determine the view parameters from six variables: the relative separation of the three constituent planes of Ultragram space ($D_{p-s}, D_{p-v}, D_{s-v}$), the number of slit holograms in the slit master (n_s), the width of the projection screen (W_p), and the width of the slit (w_s). The width of the slit master plate (W_s) is simply $w_s \times n_s$. The width of the view zone can determined[1] by:

$$W_{viewzone} \approx ([D_{p-v}/D_{p-s}] \times w_s) + ([D_{s-v}/D_{p-s}] \times W_p). \tag{2.1}$$

This gives us a maximum view zone of 900 mm.

This, however, is an inflated value. At the extreme end of the view zone, only a small percentage of the image remains visible. In Ultragram space, there is a Central View Zone, in which the information content of the image is 100% visible. Outside of the central region, the image content is reduced incrementally as the viewer moves

[1]Exact formulae for the calculations involving Halle's geometry can be found in his thesis, cited in the references. The differences from the values arrived at by the approximations used herein are insignificant for purposes of demonstration

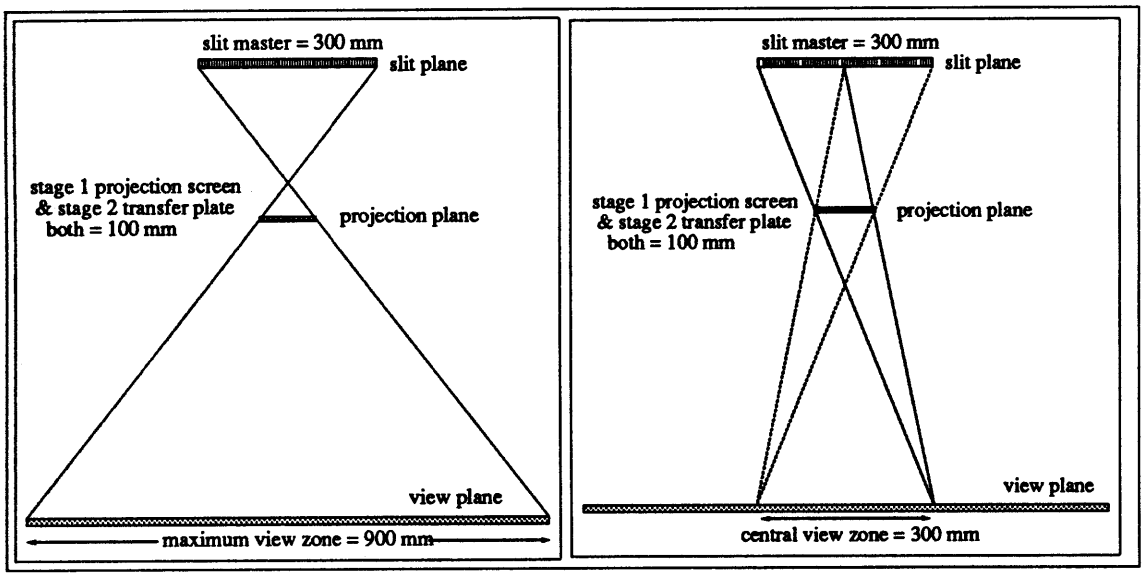

Figure 2.6: The Maximum View Zone encompasses all points at which any of the image is visible. The Central View Zone is bounded by the extreme viewpositions from which the entire image can be viewed.

to the extreme edges of the View Zone. Figure 2.6 shows a ray trace determination of the View Zone and the Central View Zone.

The Central View Zone encompasses all viewpositions in which any ray from the viewposition drawn through any point on the projection screen will strike some point on the slit master. The width of the Central View Zone can be calculated by:

$$W_{CVZ} \approx ([D_{p-v}/D_{p-s}] \times [W_s - W_p]) - W_p. \tag{2.2}$$

For our geometry, we get a Central View Zone width of 300 mm.

Lastly, we can calculate the number of discrete viewpositions from our variables.

$$n_{views} \approx n_s + [W_p/W_{p-s}], \tag{2.3}$$

where W_{p-s} is the width of the mapping of a slit onto the projection screen. We can equivalently restate equation 2.3 as:

$$n_{views} \approx n_s + [W_s \times (D_{s-v}/D_{p-v})], \tag{2.4}$$

which gives the result of 450 discrete view points.

Combining and summarizing we see that our View Zone width of 900 mm decomposes into three zones: the Central View Zone of 300 mm and two "wing zones", each also of 300 mm. Our 450 discrete views are distributed evenly amongst these three zones. In the Central View Zone, we have 150 viewpositions in which the image is fully visible. As the viewer moves out of the Central View Zone and into a wing zone, 1/150 of the image will be lost at each discrete viewposition, until at the extreme position of the View Zone, only 1/150 of the image remains visible. With individual Ultragrams, the extent of excursion into the wing zones before the image quality becomes unsatisfactory will vary, depending upon the specific Ultragram's image composition. Since the image content is, by definition, always complete within the Central View Zone, we choose to use the Central View Zone width as our figure of merit to quantify the view zone.

2.5 Conclusion

More than just streamlining the production technique of edge-lit stereograms, the plane shuffling of Figure 2.4 allows for a reduction of distortion in two-step stereograms in general, because direct illumination can be used. Direct illumination will produce a distortion-free image, whereas near-conjugate illumination, used to reconstruct traditional two-step stereograms, will introduce some small degree of distortion in the final image.

The edge-lit stereogram is but one application of the Ultragram technique. The Ultragram is a significant step forward in full dimensional imaging with interesting configurations and benefits beyond the scope of this modest introduction. Interested readers are encouraged to pursue the exhaustive treatment given by Halle in his thesis[14].

Chapter 3

Image Distortion and Compensation

3.1 Introduction

Although distortion-free stereograms are achievable in principle, our early results were in fact severely distorted. During the transfer stage, as the various image projections from the 300 slits passed through the air-tank interface, they suffered refraction-induced distortions. This is diagrammed in Figure 3.1 as a softening of the focus of the bounding pyramid of the transfer images due to refraction as they pass into the denser medium. The images then focus to a plane beyond the projection plane, and therefore will be recorded out of focus.

The defocusing of the transfer image effects both the vertical and the horizontal foci of the stereogram. Consideration of the viewing system of an Ultragram will clarify the separate distortion results for the horizontal and vertical extents.

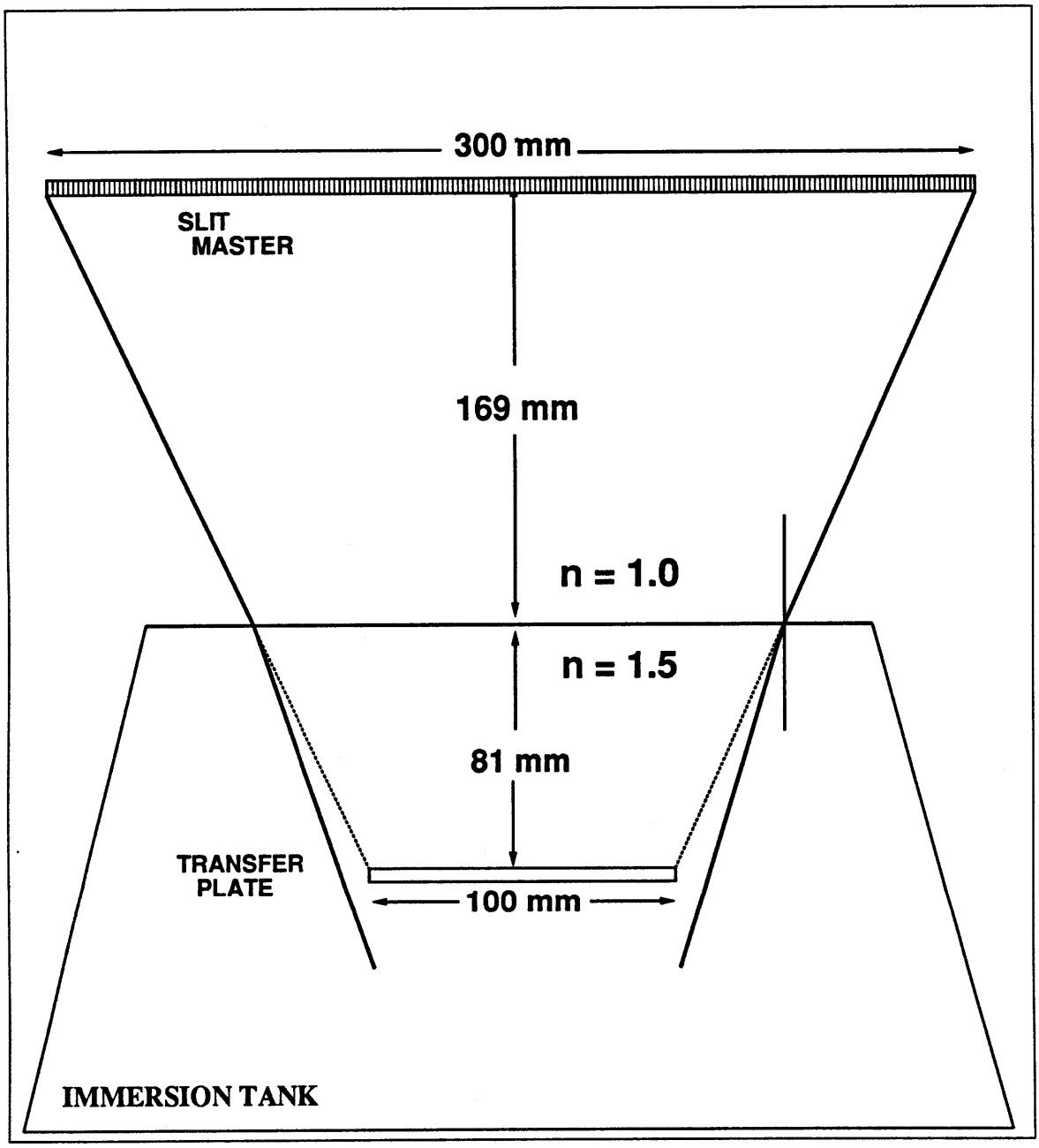

Figure 3.1: Image distortion is introduced by refraction at the air-tank interface, which changes the focus of the transfer image.

3.2 Ultragram Viewing Mechanics

The diagram of the Ultragram view geometry shown in Figure 2.4 demonstrates that the image rays that focus to a particular viewposition emanate from a large number of the slits in the slit master (in our case each viewposition receives data from 150 of the 300 slits). Each ray that focuses to the viewposition passes through a different point in the horizontal extent of the transfer plate in the Projection Plane. The viewposition represents the horizontal focus of the image data.

However, image information is viewable along the continuum of the View Plane and not just at quantized view positions. To understand the view continuum, consider a single point on the transfer plate in the Projection Plane and consider how image information from all the slits raytraces through it. For a given slit, rays will retrace to a Projection Plane point from every point across the horizontal extent of the slit. From this Projection Plane point, the ray bundle will fan out as it propagates to the View Plane. The image data from a single slit for a single image point on the Projection Plane does not focus to a single point on the View Plane, but rather projects to a "viewband" along this plane. As diagrammed in Figure 3.2, image data from adjacent slits will project to adjacent view bands, forming this Projection Plane point's viewing continuum. Each slit will project to a viewband, whose width is geometrically prescribed by:

$$W_{viewband} = w_s \times [D_{p-v}/D_{p-s}], \tag{3.1}$$

which in the example case results in a viewband width of 2 mm.

Each pixel point on the Projection Plane will be associated with its own continuum of viewbands. All viewbands, for every pixel point on the Projection Plane and for each viewband continuum, will have the same width. (This gives a linear rate

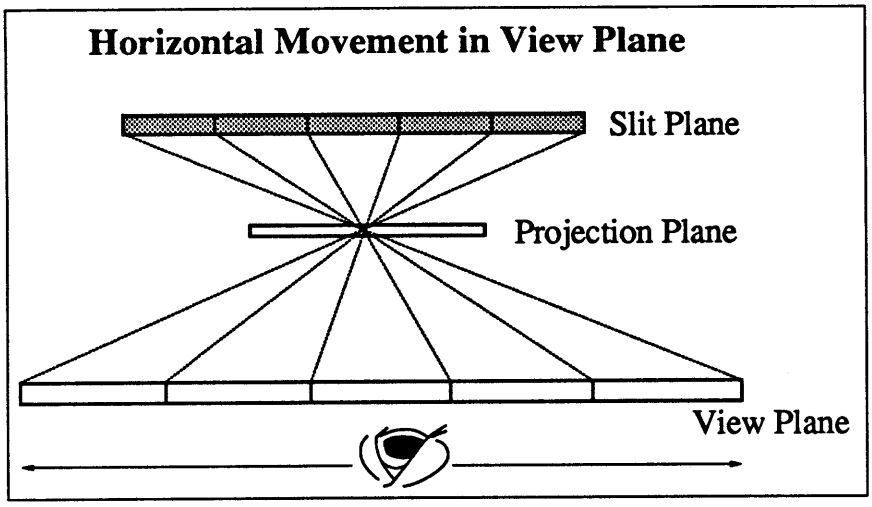

Figure 3.2: The continuous slit structure projects through pixels in the Projection Plane to a continuum of viewbands in the View Plane.

change of perspective to change of position in the view plane, satisfactorily replicating natural viewing.) The centers of viewbands for viewband continua associated with adjacent Projection Plane pixels will be offset from one another. The amount of offset will depend on pixel separation on the Projection Plane, which is itself a function of the resolution of the computer images used to record the slit master. The pixel separation (w_{px}) is simply the width of the projection screen (W_p) divided by the image resolution. The viewband center offset for viewbands associated with adjacent pixels can then be given by:

$$offset = w_{px} \times [D_{s-v}/D_{p-s}]. \tag{3.2}$$

If we use a resolution value of 600 pixels, we find our geometry gives viewband centers that are offset by 0.5 mm. Combining this result with the result from equation 3.1, we see that for our example the viewband continua for any four consecutive pixels will be offset from one another, but that the viewbands for every fourth pixel will

exactly coincide with one another. Figure 3.3 diagrams the offset of the view bands of four adjacent pixels. Viewbands, in our example, from all other pixels will map to the same location as one of the four view bands shown. The hatched area of overlap shown in Figure 3.3 is an area in which the image information for all pixels will be visible. Finally, to reconcile our two viewing systems, i.e., viewpositions versus viewbands, the center of the area of overlap of viewbands is equivalent to the point earlier defined as a viewposition.

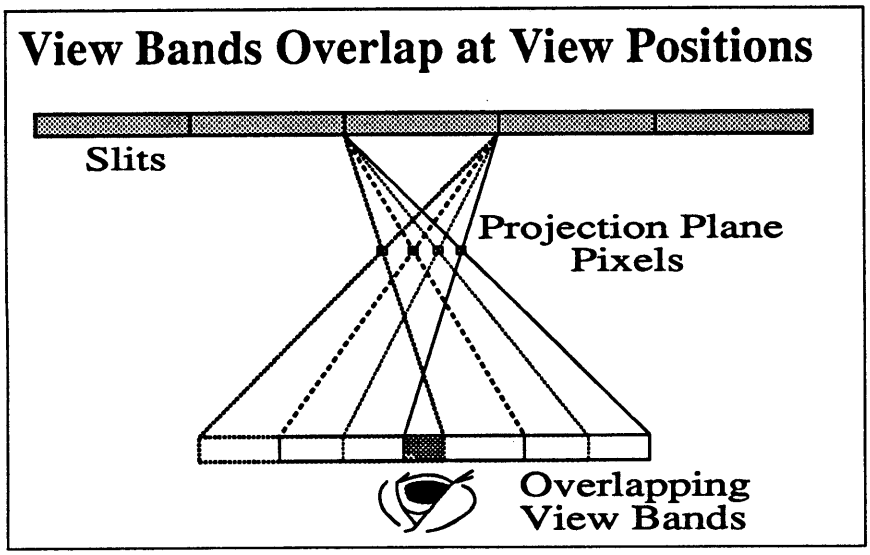

Figure 3.3: Every projection screen pixel will contribute a viewband to each viewpoint. Each viewband will map to one of four distinct positions. The hatched area marks the overlap of all viewbands associated with this viewpoint.

The mechanics of the viewing system through its vertical extent is far simpler, because Ultragrams lack vertical parallax. During the recording of the master, each image pixel will diffuse to all points through the full vertical extent of the slit in which it is being recorded. In the transfer stage, rays emanate from each of these slit points and trace back to the original point in the Projection Plane. During viewing, these rays fan out to the View Plane. Thus, as illustrated in Figure 3.4, the image content

of this pixel point will remain unchanged with vertical viewer movement through the View Plane.

3.3 Defocused Recording

There are two important aspects to the defocused recording of our transfer image. First, the improper focus results in a mismapping of the rays back from the slit master to their appropriate Projection Plane points in both the horizontal and vertical extents. In the horizontal extent, diagrammed in Figure 3.5(top), this defocused recording results in a compression of the width of viewbands, and by extension, if the defocusing operation on the ray retrace is a linear function, merely a narrowing of the viewband continua. The vertically defocused recording, diagrammed in Figure 3.5(bottom), results in the image bearing ray for a specific Projection Plane pixel mapping through a different vertical position in the transfer plate for each vertical viewposition in the View Plane. Because of this, the image will appear to move in opposition to vertical viewer movement. The second important aspect of our defocused recordings, that the causal operation, refraction, is not a linear function, complicates compensation considerations.

3.4 Distortion Compensation

A distortion compensation technique has been developed and successfully applied to edge-lit holographic stereograms. Shown in Figure 3.6, this technique approximately accommodates the effect as a shift of the plane of focus. It is based on the corrective measure that would compensate if the defocusing function were completely linear. By increasing the distance between the slit master and the tank, we can cause the width

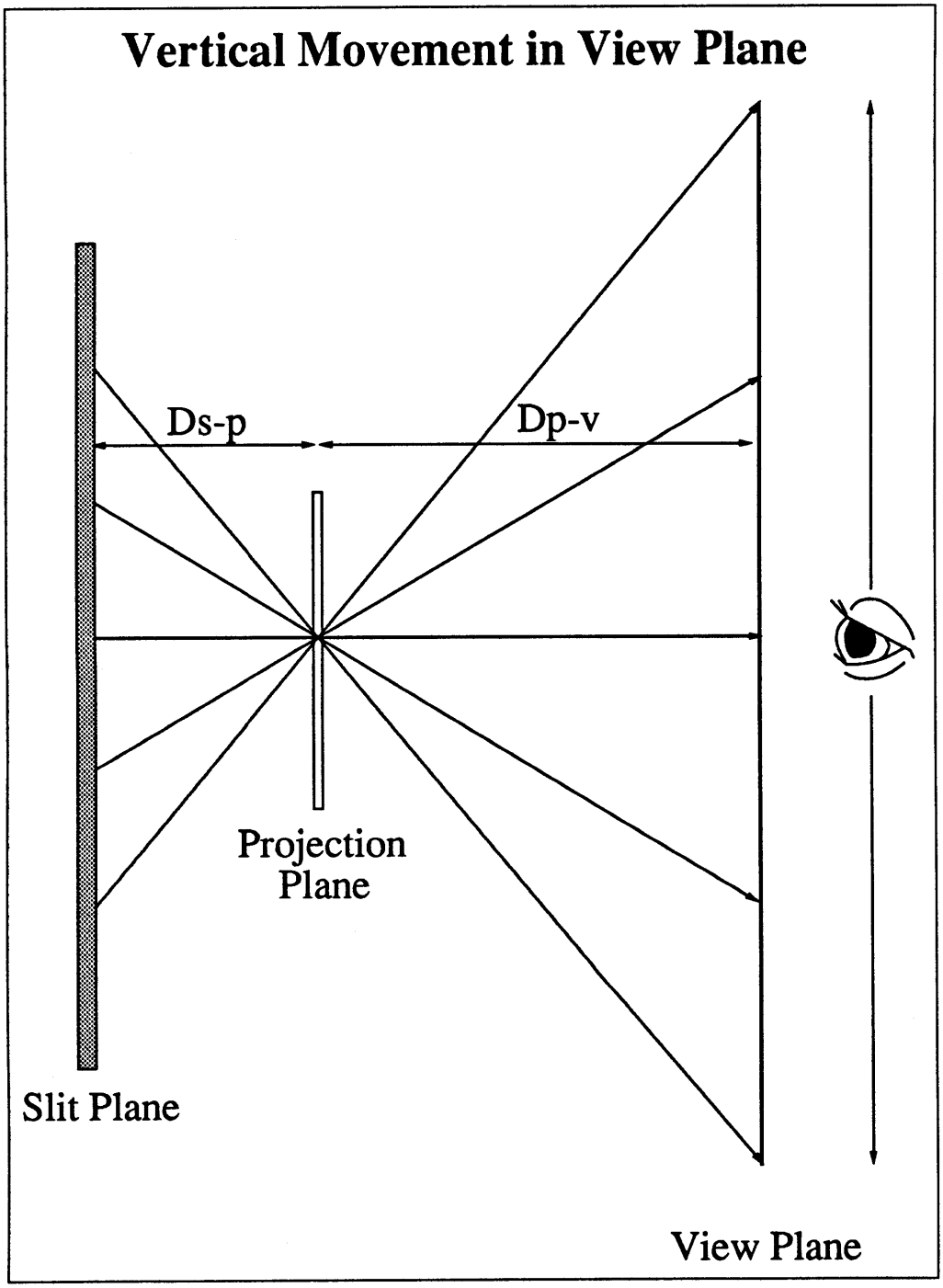

Figure 3.4: The pixel image information is unchanged with vertical movement in the View Plane because of the lack of vertical parallax.

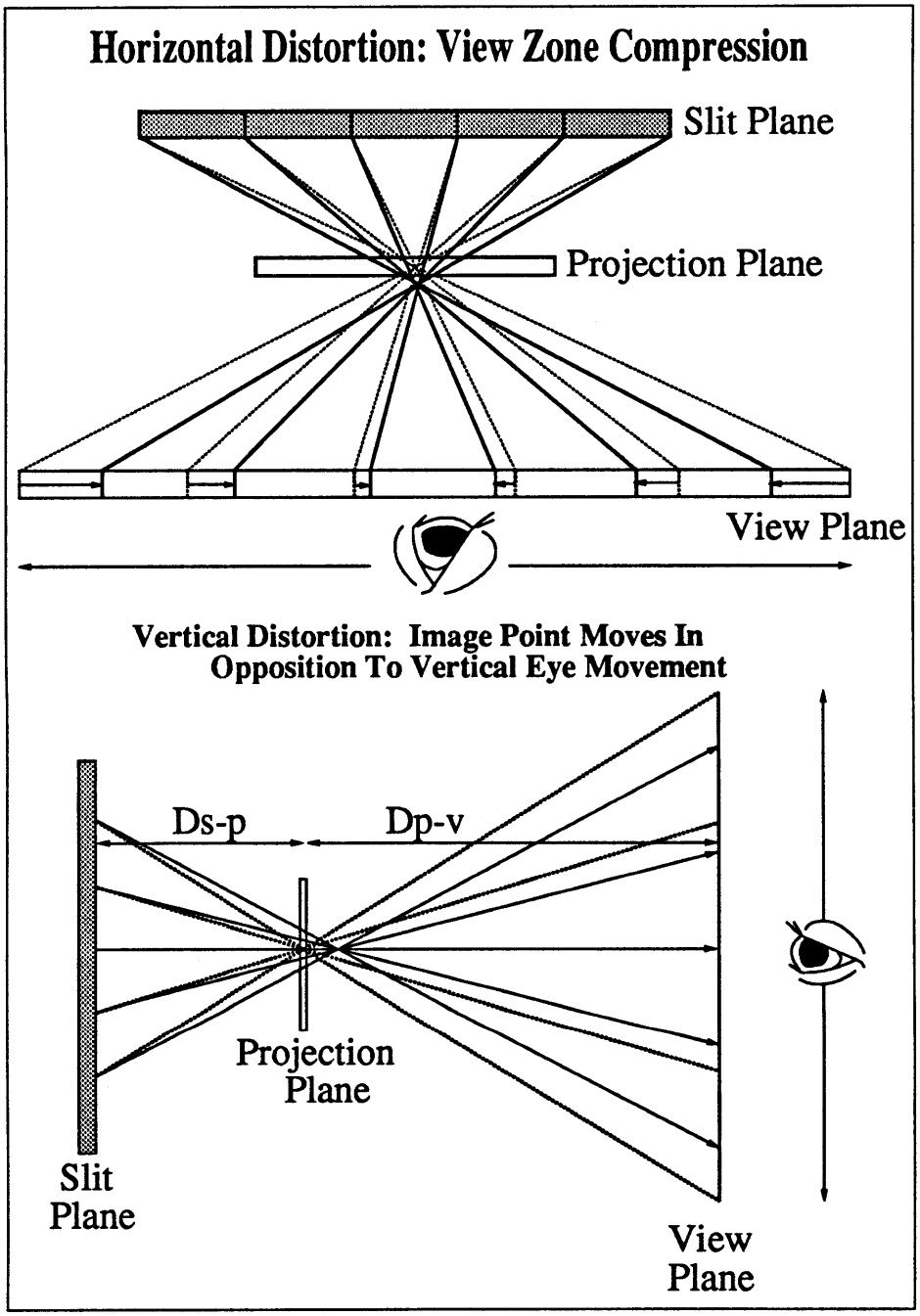

Figure 3.5: The result of rays not correctly refocusing to their Projection Plane positions is a mismapping to the View Plane, resulting in both horizontal and vertical distortions.

of the bounding pyramid to focus down to 100 mm at the plane of the transfer plate.

The appropriate increase in separation for our example is easily calculable. The angle of incidence at the interface of the edge of the bounding pyramid will remain the same (21.8°) regardless of the distance of separation, as will the transmission angle (14.4°). The depth from interface to the transfer plate inside the tank is unchanged (81 mm.). The desired distance from slit master to tank (D_{sm-t}) can then be determined from the algebraic relationship:

$$(W_s - W_p) \,/\, 2 \;=\; (D_{sm-t} \times \tan 21.8°) + (81 \times \tan 14.4°), \qquad (3.3)$$

which gives a separation value of 198 mm. We can capture the transfer image in approximate focus for our case by increasing the slit master to tank separation by 29 mm. This method results in some residual distortion. The increased separation that compensates for the extremes of the transfer images' bounding pyramid assures exact compensation only for the interior rays that strike the interface at the same angle as the edges of the bounding pyramid. All other rays will suffer a certain degree of error in their remapping onto the Projection Plane for recording in the transfer. Moreover, the residual distortion will have both horizontal and vertical effects.

3.5 Residual Distortion

Because the Ultragram is a horizontal-parallax-only device, we are primarily concerned with horizontal distortion. The effect of the residual horizontal distortion can be seen from separate analyses of various elements of the Ultragram viewing system that have been introduced in this paper. Determination of deviations in the size of viewbands along all continua will demonstrate the degree of non-adherence to the

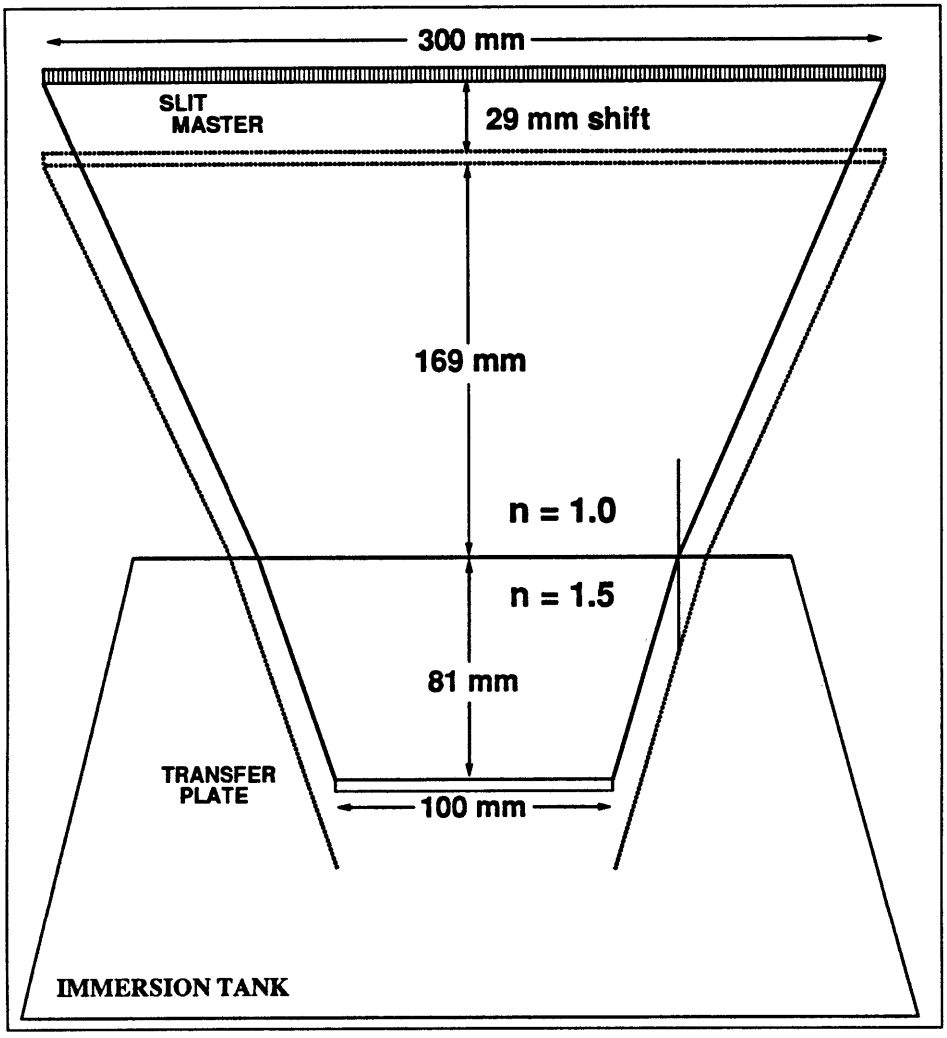

Figure 3.6: Shifting the plane of focus, by increasing the distance separating the slit master and tank, approximately accommodates the effect of refraction.

linear rate change of perspective to movement through the viewplane. Analysis of the overlap of viewbands at sample viewpoints will reveal the integrity of image data at these viewpoints, as well as changes in the viewing transition in passing through adjacent viewpoints.

Each pixel point on the Projection Plane will be associated with its own viewband continuum. The continua of all pixel points will be identical in structure, but offset from one another. For each continuum, the viewpoint directly across from the continuum's pixel point will serve as a center of symmetry for the distortion of the continuum. And the distortion for each continuum will be identical, because the angle of incidence on the distorting interface of the limiting rays for each positional viewband in every viewband continuum is identical. The distortion effect on a continuum will be a narrowing of the width of viewbands along the extent of the continuum. The narrowing will be weakest at the center of symmetry for the viewband and will increase nonlinearly moving away from the center. Figure 3.7 shows a graph of this nonlinear narrowing along the continuum for the case of uncompensated distortion. At the center of the continuum the viewband width is 108μm smaller than an undistorted viewband. At an extreme of 200 mm from the center of the continuum, the viewband has been reduced by 134μm.

For the case of continua after this shift-of-focal-plane compensating technique had been applied, calculations were performed to determine residual refraction-induced width-change for each of the viewbands associated with the continua that blanket the Central View Zone. The results, graphed in Figure 3.8 are highly significant for two reasons. The range of viewband width changes are a full order of magnitude smaller than for the uncompensated case. Moreover, the viewbands of a continuum now have their narrowest member at the center of symmetry and increase in width along the continuum. At 114 mm from the center, the viewbands in the continuum pass from being smaller than an undistorted viewband to being larger. Instead of growing nar-

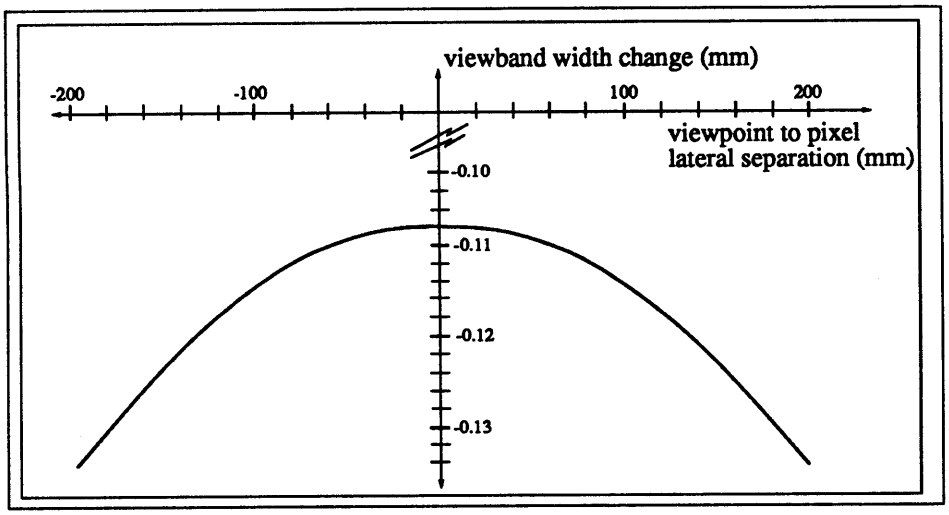

Figure 3.7: This graph plots the change of viewband width as a function of its distance from the center of the continuum for the case of uncompensated distortions.

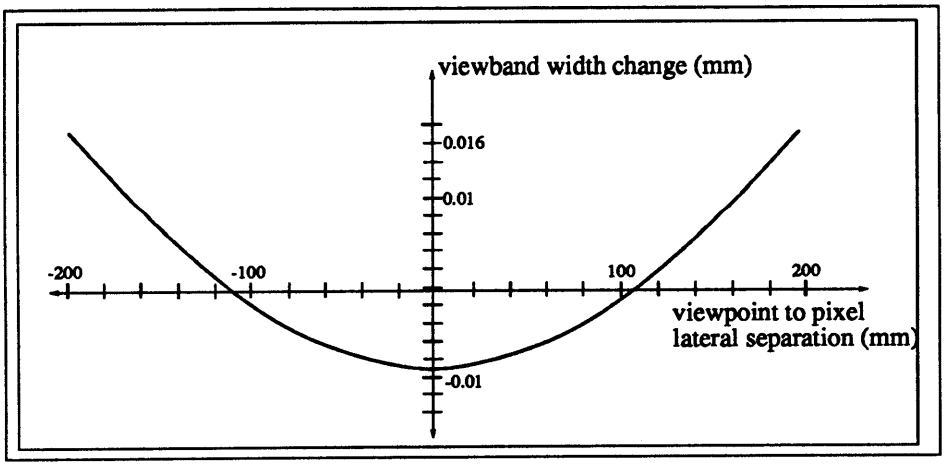

Figure 3.8: This graph plots the change of viewband width as a function of its distance from the center of the continuum for the case of compensated but residual distortion.

rower towards the extremes of the continuum, the viewbands increase in size, so that the range of values now hovers on either side of the undistorted viewband width of 2 mm. The tremendous significance of this will be evident momentarily.

In the compensated case, the maximum deviation (from the prescribed 2 mm width of the viewbands for our example) for any single viewband was 16μm. More importantly, the maximum difference in width for any adjacent viewbands along a continuum was a mere 0.2μm. Fortunately, because of the microscopic nature of this difference, the deviation from perfect linearity of the rate change of perspective view is too subtle to be observable.

The overlap of viewbands at specific viewpoints reveals the strongest effect of our residual distortion. The earlier illustration of the overlap of viewbands at a viewpoint, Figure 3.3, showed four distinct viewband positions. In the case of an undistorted Ultragram with our geometry, each viewband continuum will map a viewband onto one of these four positions. A viewer moving from one viewpoint to an adjacent viewpoint will experience a change of perspective that is divided into four interleaved sets. The crossing of each of four evenly spaced boundaries in the region between viewpoints will result in a change of one-quarter of the image pixels in an interleaved manner. The distortion from refraction variously shifts the mapping of these viewbands so that the component viewbands of each of these four sets will map slightly offset from one another rather than atop one another. This offset does not degrade the viewing experience, per se, because ocular integration smoothes the visual effect of the staggered data change. However, if the offset of viewbands becomes large, then the overlap of all viewbands, shown in Figure 3.3 as the criterion which defines a view position, may not occur and the image data at a viewposition will then become a composite of data intended for disparate viewpositions.

Here we see the significance of the difference in the change of viewband width

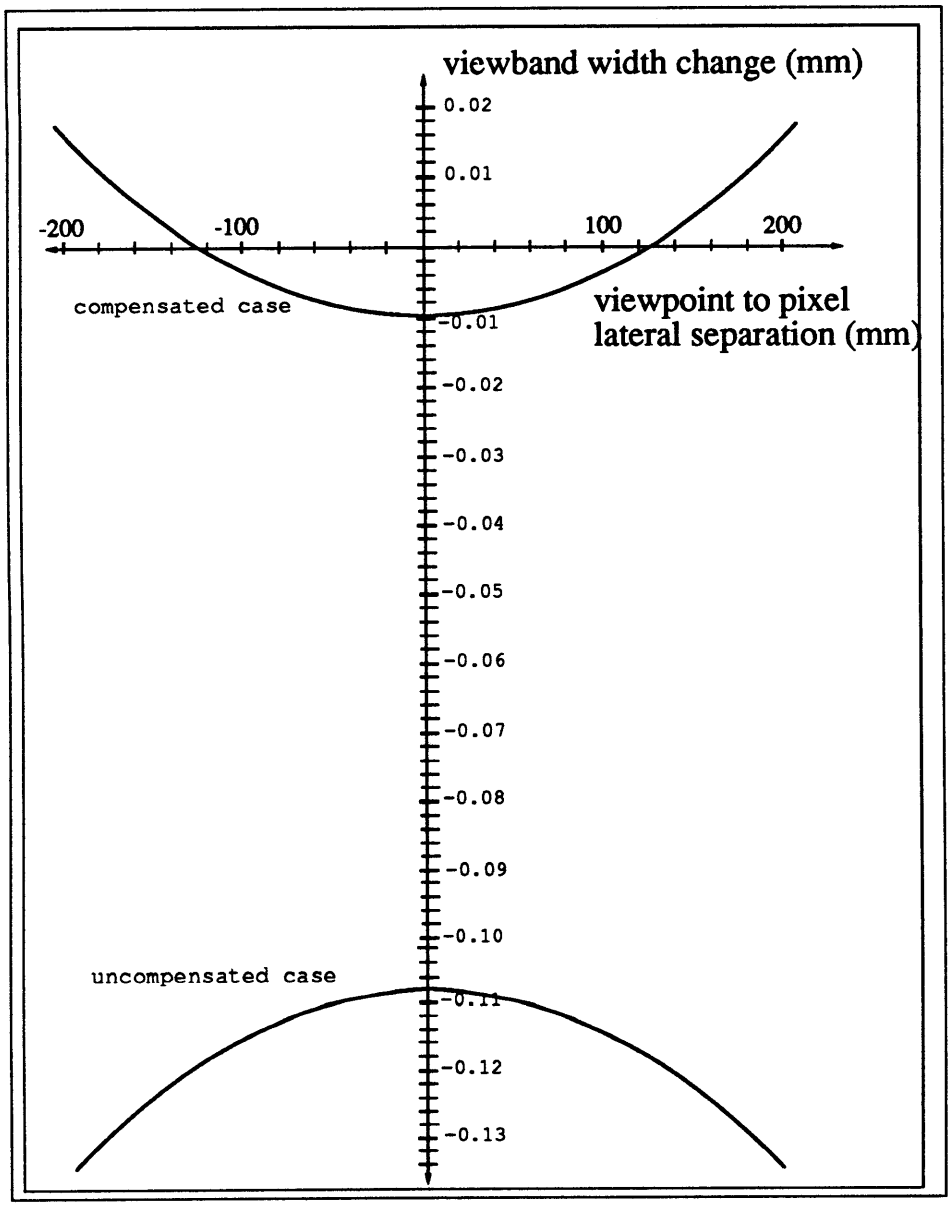

Figure 3.9: This graph of the viewband width changes along the continuum for both the uncompensated case and the compensated case displays their differences in both magnitude and polarity.

versus continuum position of our uncompensated and compensated cases. The two cases have been graphed together in Figure 3.9 to clearly demonstrate the difference of range between them. The data integrity of a viewposition is contingent upon the viewposition being embraced by all of the viewbands that would map to it in an undistorted case. The mapping of viewbands along the View Zone can be thought of metaphorically as a convolution of a view continuum with itself. The symmetry of the continuum around its central viewband takes care of the sign flip for one of the convolved continua. In the convolution operation, the stationary continuum can be thought of as representing the central continuum, while the sliding continuum can be thought of as representing the continuum for the succession of all pixel points on the Projection Plane with each incremental shift. Each viewposition will, during this operation, have mapped to it its contributed viewband from each continuum. The integrity of the viewposition will depend upon the accuracy of the viewband mapping during this convolution.

The accuracy of this viewband mapping will depend directly on the widths of the viewbands along a sample continuum. The amount of mismapping of a specific viewband from a continuum to a viewposition will be equivalent to the distance this viewband has shifted along its continuum due to the influence of the distorting function. The amount of shifting will be an offset equal to the integration of all of the changes in width of all of the viewbands from the center of the continuum out to the specific viewband in question. Since the viewing system of a stereogram is discrete, the integration is actually a summation of the discrete viewband-width-change values.

Figure 3.10 displays a graph of the positional shift of the viewbands along a continuum for the uncompensated case. Because the change in viewband width is a monotonically decreasing function (see Figure 3.7) the positional shifting for viewband position is a monotonic function. For negative continuum positions the positive shift

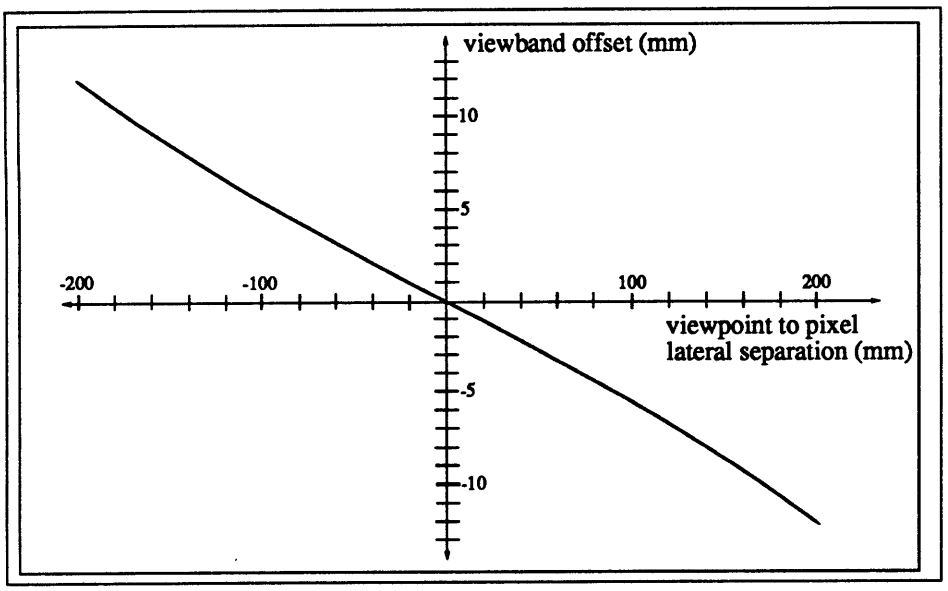

Figure 3.10: The positional shift of viewbands along the continuum in the uncompensated case is a monotonic function.

and for positive continuum positions the negative shift both represent a movement towards center and hence a narrowing of the width of the total continuum. Because the average value for individual viewband contraction is in the range of 120μm, at the extreme position, the 100th viewband at a distance of 200 mm from the center, the accumulated shift is almost 12 mm. The amount of shifting for a viewband that would be tolerable before effecting the integrity of a viewposition is 0.25 mm. Obviously, the further the shift is out of bounds, the greater the viewing aberration. With a shifting of 12 mm, we get viewpositions that have data mapped to them that are intended for 6 distinct viewpositions. The result is a severe distortion, similar to a bending of the image, so that internal parts of the image are shifted inward moderately, while extreme positions on the image are shifted inward greatly.

The positional offset for a viewband along a continuum for our compensated case is shown in the graph in Figure 3.11. The fact that the average width-change for

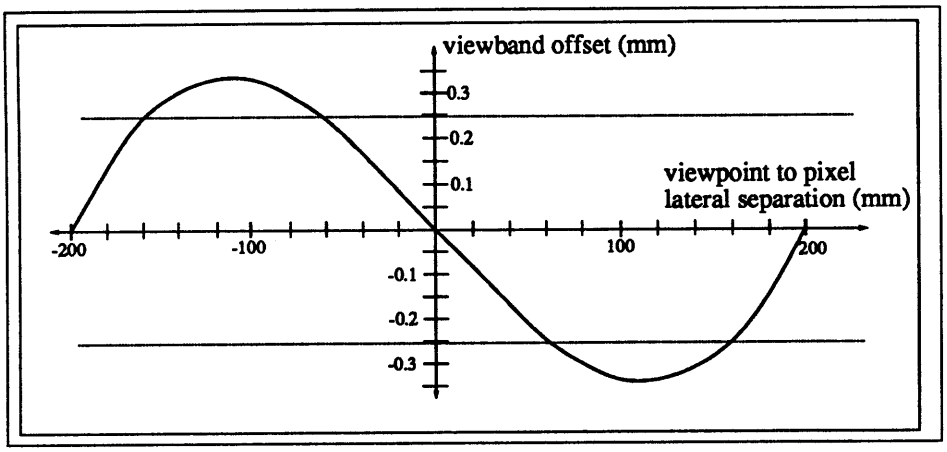

Figure 3.11: The positional shift curve for our compensated case contains a turning point because the size of individual viewbands changes from smaller than to larger than the norm along the continuum.

individual viewbands is an order of magnitude smaller than for the uncompensated case means that the cumulative positional shift for the extreme positions will also be an order of magnitude smaller. Moreover, the shift-of-focal-plane compensation technique reverses the direction of the viewband width-change curve (Figure 3.9), resulting in a change along the continuum of viewband size from smaller than the undistorted norm to larger than this norm. The summation that determines the positional shift for extreme viewbands along the continuum will now contain both positive and negative terms and the positional shift function will not longer be monotonic, but as graphed in Figure 3.11, will include a turning point so that at the extreme viewband the positional shift has been completely compensated for and this viewband maps exactly to where it would in the undistorted case. A comparison of the uncompensated and the compensated positional shifts is shown in the graph in Figure 3.12.

The viewing effect of the residual distortion in our compensated edge-lit stereogram can be understood by consideration of the graph of its positional shift(Figure 3.11).

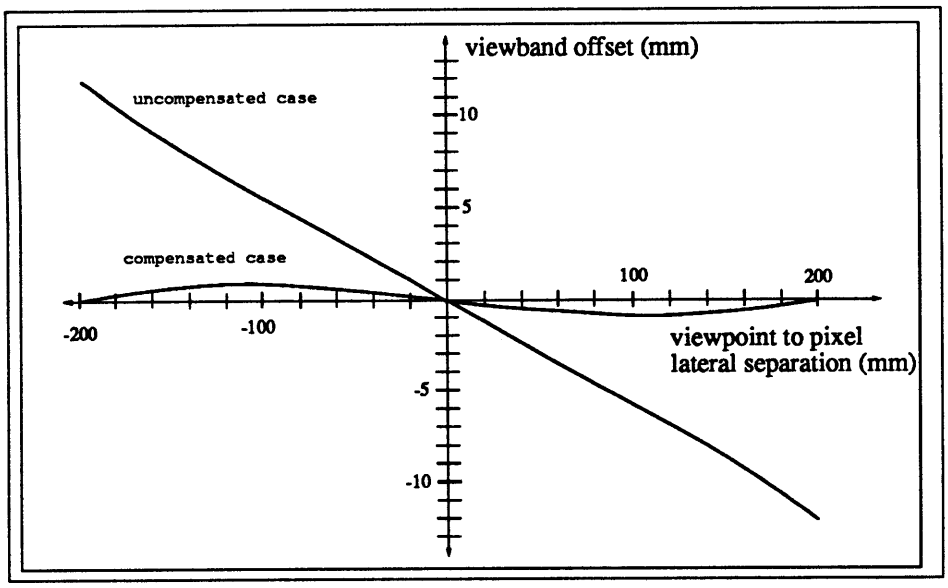

Figure 3.12: This graph displays the great difference of the positional shift curves for the compensated and uncompensated cases.

On the graph, the central zero-crossing is a natural consequence of the fact that a ray with no horizontal component will be perpendicularly incident at the interface and therefore will experience no refraction. The zero-crossings at positive and negative 200 mm result from our compensation; these rays will be incident on the interface at the same angle as the edge of the bounding pyramid (see Figure 3.1). Other critical points on the graph are at:

- ± 61 mm : At this point the offset becomes greater than 0.25 mm. This is the critical limit for viewpoint integrity. Offset greater than 0.25 mm means that image data will map to a viewposition from an incorrect slit location.

- ± 114 mm: The value of offset reaches a turning point. Refraction wants to drive the offset in one direction and our compensation exerts a force to drive the offset in the other. At this turning point the respective forces are balanced.

- ± 157 mm: The offset passes to a value of less than 0.25 mm, entering a second region of correct mapping.
- ± 200 mm: This zero-crossing represents the maximum pixel point to viewposition separation for our example.

The viewing effect of uncompensated shifting of the viewband due to refraction would be a monotonically growing curvature of the projection plane image that can be modeled as one-dimensional pin-cushion distortion. Our compensation technique assuages this distortion by introducing what can be considered a one-dimensional barrel distortion.

The result in viewing is imperceptible. The minimal residual distortion results in no degradation of viewing in the horizontal extent. A photograph of the image of the edge-lit stereogram can be seen in Figure 3.13

The distortion in the vertical extent is visually apparent. The result in viewing is a small rolling of the image away from the direction of vertical viewer movement. However, because this edge-lit stereogram is a horizontal-parallax-only device, and is designed for horizontal viewer movement through the view plane, the vertical effect only slightly mitigates the overall viewing satisfaction.

3.6 Conclusion

A simple compensation technique has been developed, involving shifting the plane of focus of the transfer image by altering the geometrical relationship of the Slit Plane and the Projection Plane preparatory to the transfer step. The simplicity of the the shift-of-focal-plane technique allows Ultragram masters, recorded according to the general Ultragram algorithms, to be transferred into the edge-lit format. While the

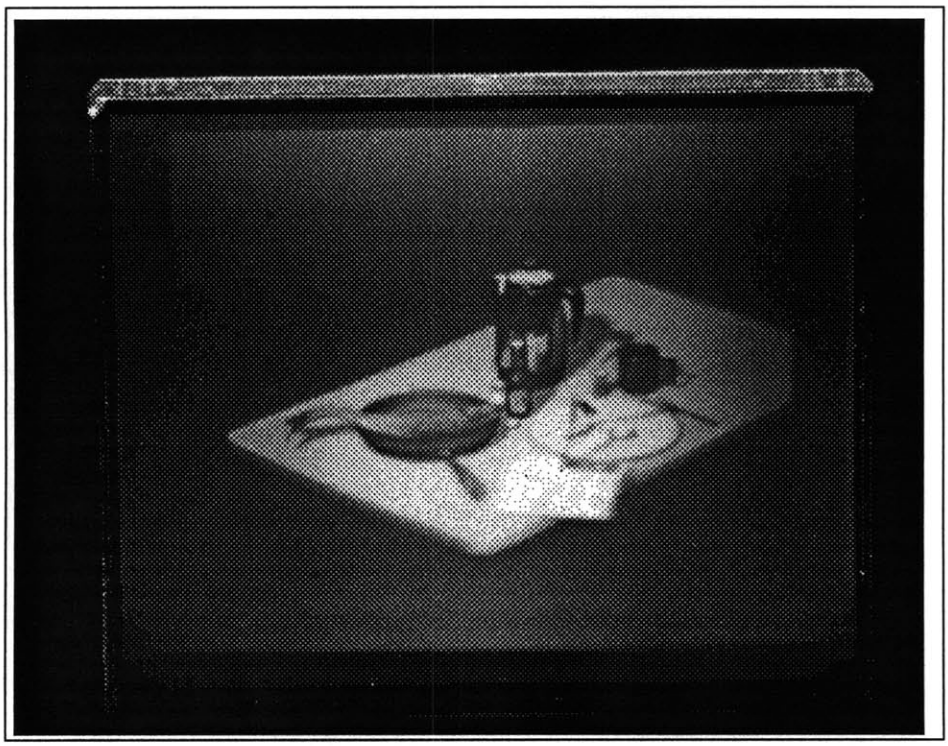

Figure 3.13: A photograph of the final edge-lit stereogram image.

final image of the edge-lit stereogram is visually gratifying, there are minor residual distortions. In the next chapter, we will look at the problem of refractive distortions from a second perspective, in an attempt to develop a superior compensation technique.

Chapter 4

A Second Compensation Technique : An Analysis and Proposal

4.1 Introduction

While the compensation technique that was detailed in the previous chapter provided high quality edge-lit holographic stereograms, there are two aspects of its results that are less than wholly satisfying. First, some degree of distortion remains. And even though the resultant images do not apparently suffer from this small residual distortion, it would be preferable to be able to produce images that were totally distortion-free.

The second less-than-totally-satisfying property of the images produced by our previous compensation method is the rolling of the image accompanying vertical

viewer movement in the View Plane. Recall that this rolling resulted from image data vertically mismapping to the transfer plate because of refraction experienced entering the immersion tank.

In this chapter, we will detail an analysis that was performed in an attempt to improve the final image. The result is a proposal for an altered recording technique that solves the problem of vertical focus on the transfer plate, but does not result in a distortion-free image in the horizontal extent.

4.2 Matching Optical Paths

The analysis begins with the recognition that the distortion in the edge-lit stereogram, in both the vertical and horizontal extent, results from an optical path mismatch. The optical path from the Slit Plane to the Projection Plane is different during the mastering and the transfer steps. This difference is, of course, the inclusion of the half of the immersion tank that lies between these two planes during the transfer stage. Inclusion of an element of matched size and refractive index to, and occupying the same position as the half-tank during the recording of the slit master would match optical paths for both stages. As diagrammed in Figure 4.1, this could be accomplished using a passive optical element, such as a block of glass.

In the vertical extent, this would automatically correct the focus. All rays would travel identical optical paths from diffusing screen to slit master during mastering and back from slit master to transfer plate during transfer. As diagrammed in Figure 4.2, the refraction experienced upon entry into the tank would match exactly the refraction experienced upon exiting the compensating element. This would result in a correct remapping of the image data in the vertical extent.

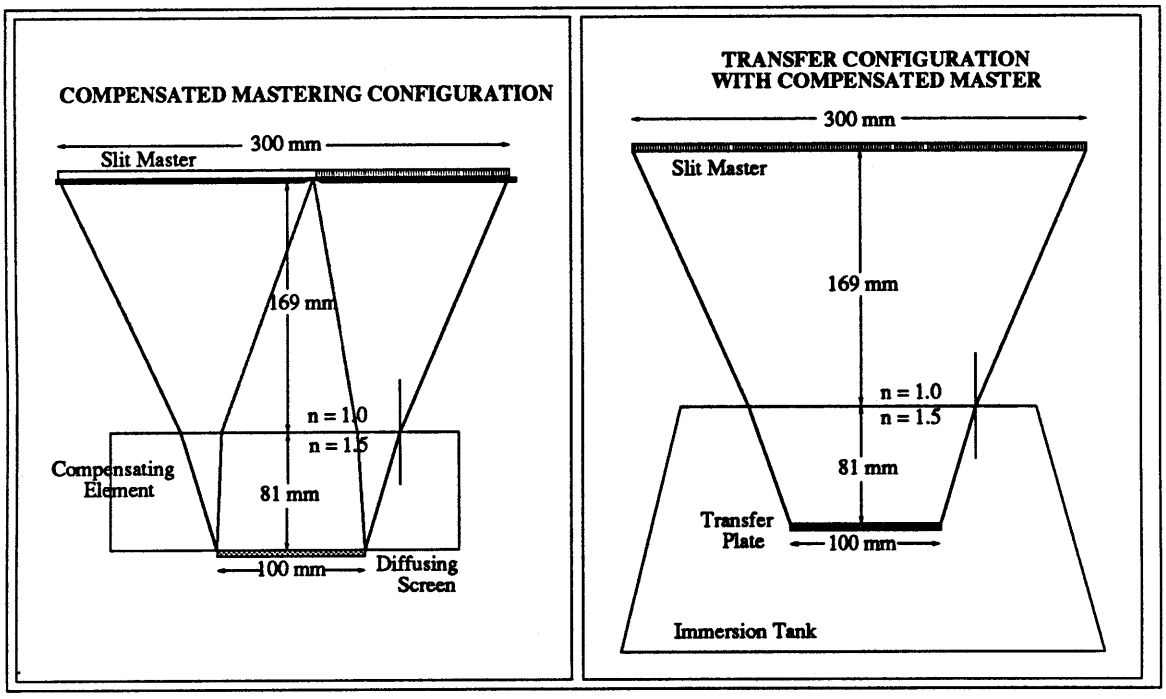

Figure 4.1: Inclusion of a passive compensating element in the mastering stage, matches the the optical path between the slit and projection planes for the two stages.

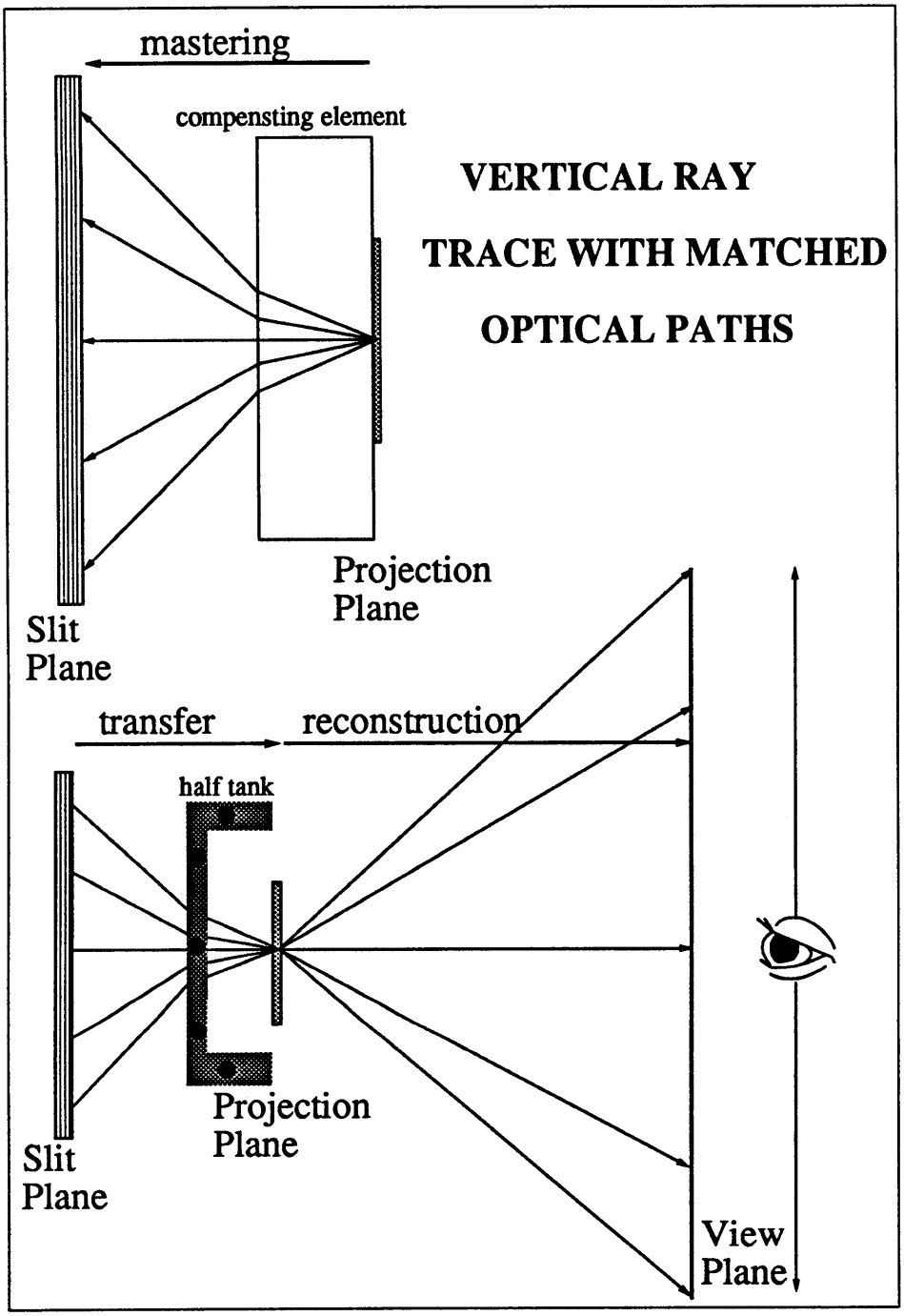

Figure 4.2: The matching of optical paths results in image data correctly remapping to the projection plane, thereby eliminating the image roll error that results with the original compensation method.

The case of the horizontal mapping is far more complicated because of horizontal parallax. To be free of distortion in the horizontal extent, Ultragrams must satisfy two criteria. We will elucidate the logical underpinnings of these two criteria, by briefly reviewing the Ultragram's information storage and image reconstruction techniques.

4.3 Criteria for Distortion-Free Viewing

With the Ultragram, as with all stereograms, there is a one-to-one correlation of perspective views to viewpositions. Unique to the Ultragram, this correlation does not extend to a similar correlation between perspective views and storage slits. Rather, the perspective view matched to a viewposition is sliced up by the Ultragram's predistortion technique and is stored in an array of slits. The appropriate storage slit for each pixel of the image can be easily determined by tracing a line from the viewposition through the pixel to the Slit Plane. This line will terminate within the storage slit appropriate for the pixel. Figure 4.3 diagrams the slicing of a perspective image and matching the slices with an array of slits. After the perspective images for all viewpositions have been sliced and matched to storage slits, new images are composited from the perspective slices that have been matched to each slit. These newly composited images are used to record the slit master.

The first criterion for distortion-free imaging involves the next production step, the transfer stage. During the transfer stage, the images from all slits are simultaneously multiplexed onto the transfer plate. If the optical paths are identical for both the mastering and transfer stages, all of the image pixels will remap to their original Projection Plane locations. The recording, during the transfer stage, of the image pixels in their correct Projection Plane positions is the first criterion for distortion-free images. Our original shift-of-focal-plane compensation technique failed to satisfy this

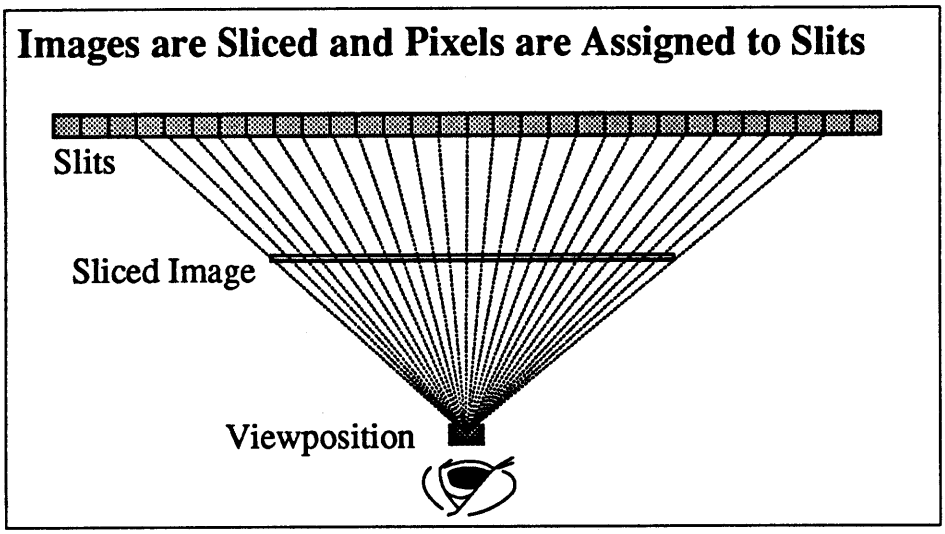

Figure 4.3: Appropriate storage slit assignment is determined by slicing the image, tracing from a viewposition through the image to the Slit Plane.

criterion. By matching the optical paths of the two recording stages, like the vertical extent, the image data will remap correctly in the horizontal extent, satisfying this criterion.

The second criterion for undistorted images involves reconstruction of the image for viewing. The requirement that all of the image data trace back to its correct viewposition during viewing is the second criterion for undistorted images. The use of a compensating element in the mastering stage to match the optical paths of the two recording steps results in the failure of this second criterion.

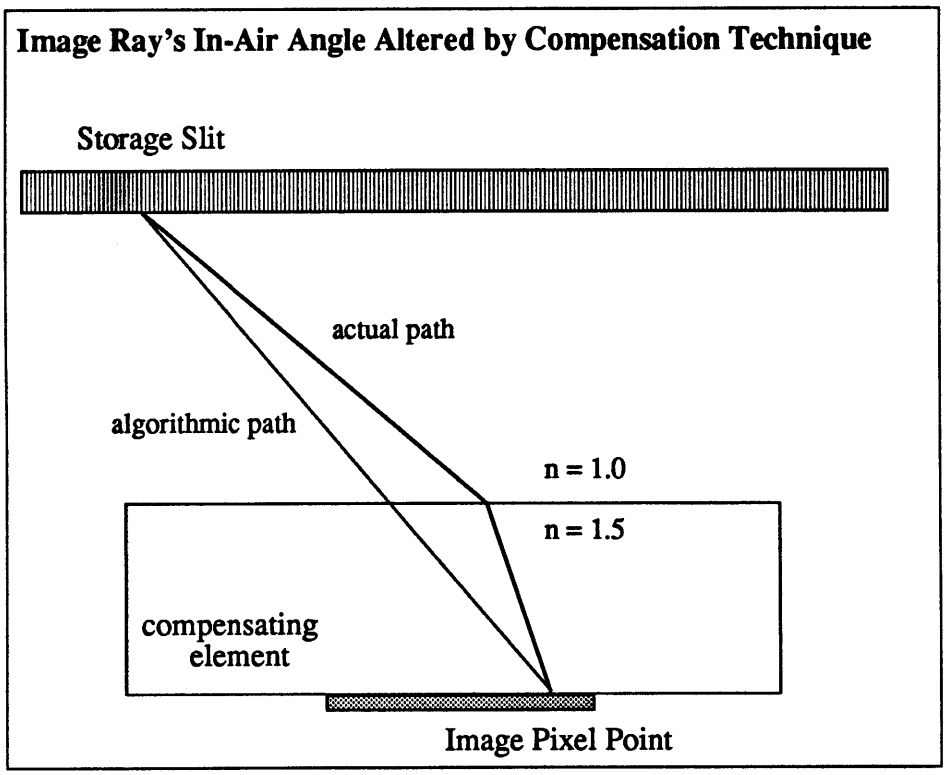

Figure 4.4: The ray from image pixel to slit is now broken into two segments. The angle of the segment in free space is different from the value used in the Ultragram algorithms.

4.4 Distortions Introduced by the Compensating Element

When a compensating element is used in the recording of the slit master, image rays to be recorded no longer impinge on the slit master at their algorithmic angle. Recall that a straight line had been used to match image pixels to their storage slit. In Figure 4.4, this line is referred to as the algorithmic path. Also shown in this figure is the more obtuse path the ray will actually travel, broken into two parts, joined at the refractive vertex where the ray emerges from the compensating element. There is a clear angular disparity between the algorithmic path and the in-air portion of the actual path.

During reconstruction, pixels' image rays will emerge from the transfer plate into air at the same in-air angle that the rays traveled during the mastering and transfer stages. As shown in Figure 4.5, because this angle no longer matches the algorithmic angle, these rays will no longer trace to the algorithmic viewpositions. The angle the rays actually travel in air is larger than the algorithmic angle. Image rays will therefore map beyond their intended viewpositions, resulting in a stretching of the view continua.

In developing a technique to adjust for this mapping error, we are bound by a new constraint. The fundamental principle of the matched-optical-paths technique is that the optical path between the Projection Plane and the Slit Plane is identical for the mastering and transfer stages. This precludes the kind of adjustment we used in the shift-of-focal-plane technique, because it introduced a difference in the separation between these two planes during the two recording stages. Any mismatching of the optical paths between stages, will result in a violation of first criterion for distortion-free images.

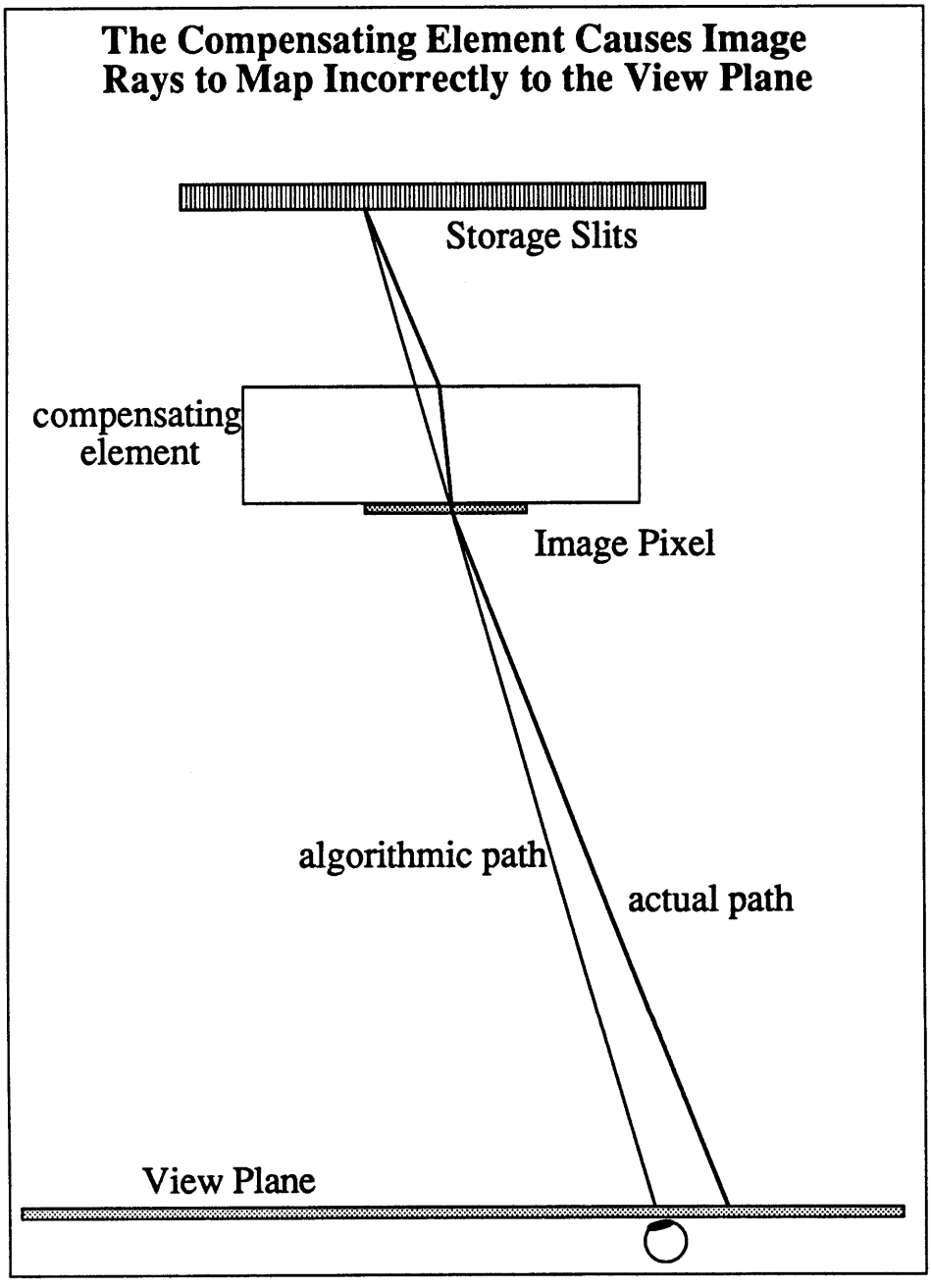

Figure 4.5: The compensating element introduces angular disparity during recording, which results in incorrect image mapping to the View Plane.

4.5 Investigation of Slit Reassignment

Because the mismapping error is the result of a change in the in-air angle, this angle becomes the focus of our attempt to develop a corrective procedure. Pairing pixel points with new slit locations chosen so that the resultant in-air angle during recording matches the the algorithmic angle would, in principle, correct this mismapping to the View Plane during reconstruction, while maintaining the integrity of the mapping to the pixel locations during the transfer step. In other words, through this slit reassignment we could simultaneously satisfy both criteria for undistorted recording. Figure 4.6 displays a comparison of the algorithmic path, the path to the original slit along the matched optical path and the path to the reassigned storage slit. Note that the in-air portion of the raytrace to the new slit travels parallel to the algorithmic path.

The new slit assignments can be arrived at by either of two methods. Working from the recomposited images matched with specific slits, we can calculate the appropriate new slit for each pixel of each image such that the image rays will travel at correct angles during recording. Once the new slit assignments are generated, a new composite image can be generated for each slit from its new component pixels. We can arrive at the same result by backing up one step and performing a new "slice-and-dice" on each viewpoint's perspective image, incorporating the compensating element into the process.

Figure 4.7 diagrams this new slicing of a representative perspective view. Rays are traced from the viewposition through the Projection Plane and the compensating element to the Slit Plane. The twice refracted path shows the path our image data ray will travel in each of the three transits of concern, i.e., from projection to slit during mastering, from slit to projection during transfer, and from projection to view during reconstruction. In Figure 4.8, the slicing of our sample image is compared with

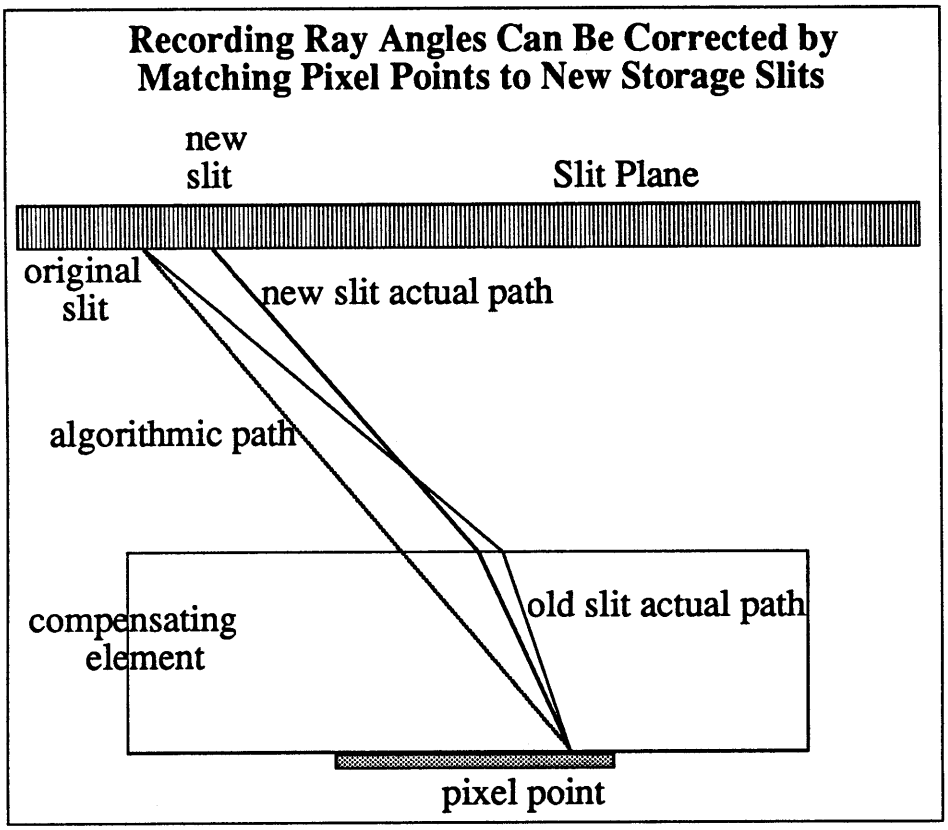

Figure 4.6: By assigning pixels to new recording slits, the ray angle during recording can be matched to the algorithmic angle.

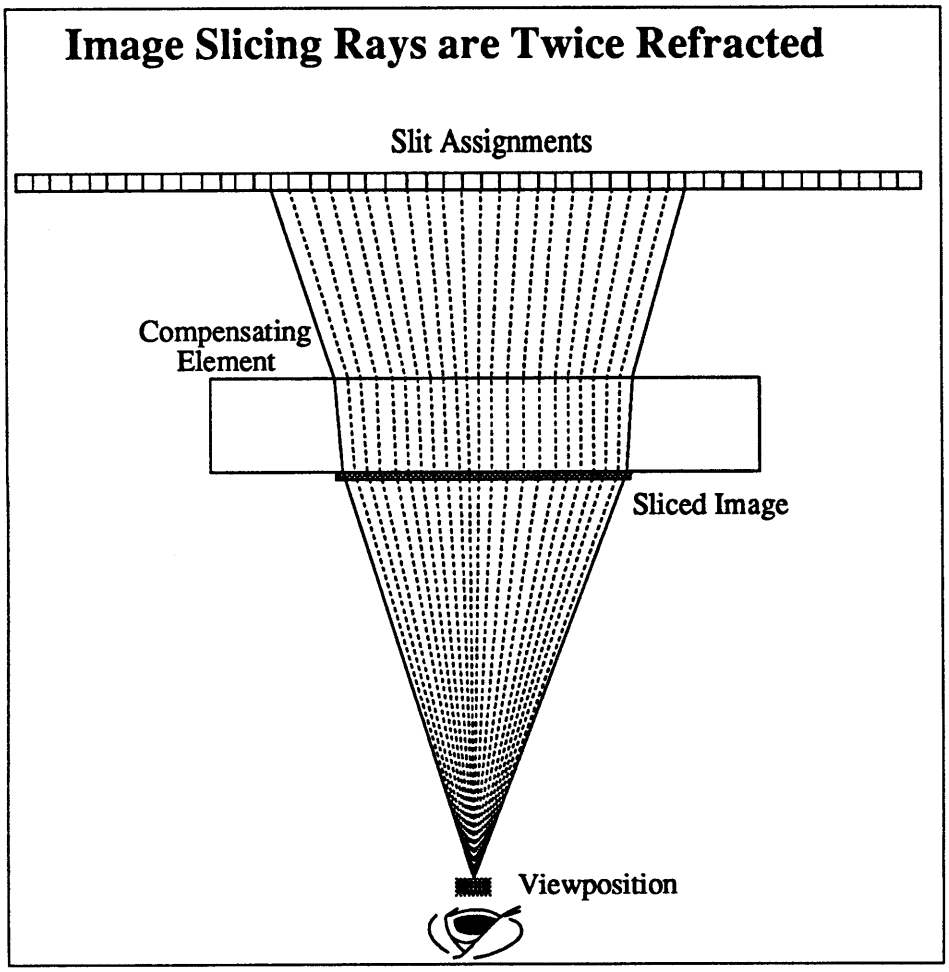

Figure 4.7: New slit assignments can be made by tracing the rays as before. Now, however, the slicing rays will be twice refracted, entering and exiting the compensating element.

the slicing for the Ultragram without the compensating element included. Clearly, the effect of the compensating element is to compress the image projection onto the slit plane, thereby trying to store the image in a reduced number of slits. This means that a greater number of pixels must be stored in each available slit. This in turn leads to competition amongst pixels for inclusion in specific slits.

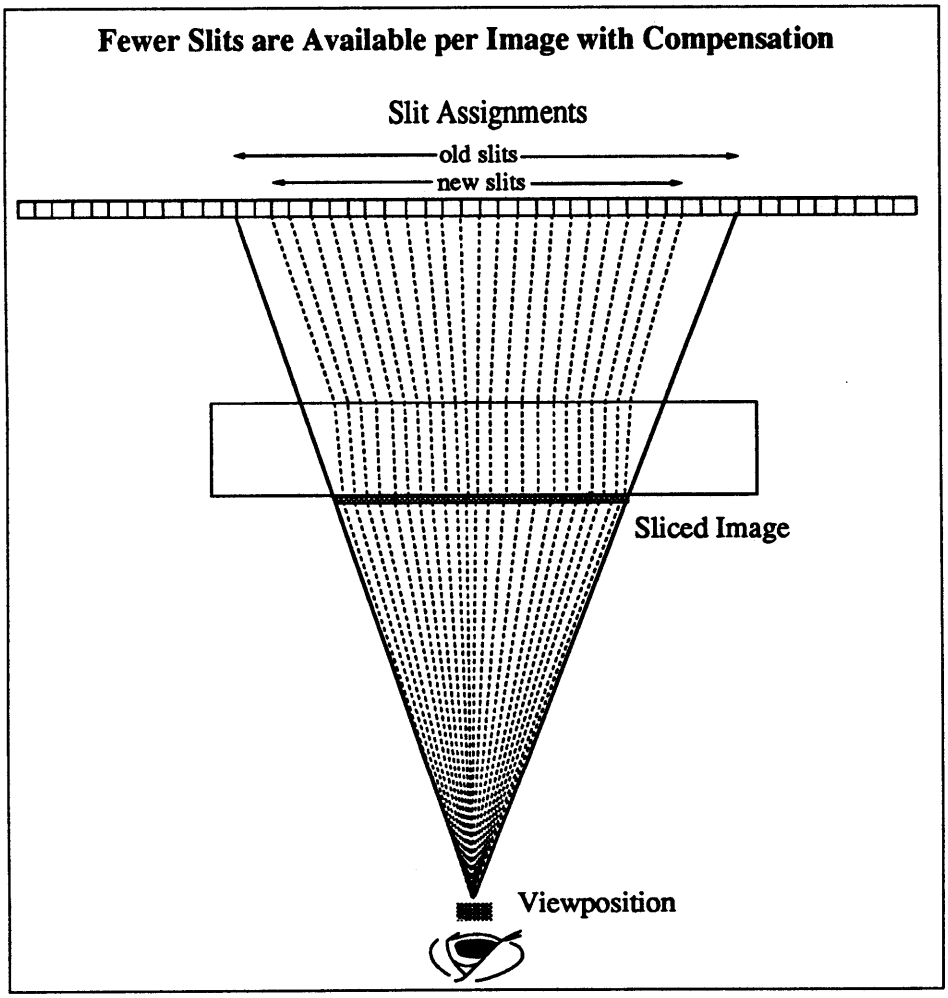

Figure 4.8: The range of slits available for pixel storage is significantly reduced because of the narrowing caused by refraction.

When slit reassignments are mathematically calculated, the competition for slits

is confirmed. Whereas, originally a perspective image was stored in 150 slits, the slit reassignment algorithm calls for an image to be stored in 144 slits. There is no way to enact this condensed storage without the loss of image data.

If, however, we can project the perspective images onto the slit plane with a coverage of 150 slits, without violating the constraints of the matched-optical-paths technique, we may end up with a viable compensation technique. Observing in Figure 4.7 that the perspective image projection is still diverging as it impinges on the Slit Plane, it becomes obvious that if the slit master were further away, the projection would spread across more slits. At some distance the projection will cover a full 150 slits, and there will be sufficient storage available to handle all the pixels.

4.6 Optimization

When we calculate the increase in the separation from the compensating element to the Slit Plane to provide sufficient slit storage for our perspective views, we discover that a range of separation values exist, dependent upon the specific viewpoint whose perspective image is used. For some of the values in this range, pixel competition continues, but for pixels that map to positions well outside of the Central View Zone, and, therefore, outside of our range of concern.

When the compensating element to slit master separation is increased to provide sufficient slit storage for the perspective images, it becomes unnecessary to reassign any pixels to new slits. All of the images composited by "slice-and-dice" according to the standard Ultragram algorithms can be recorded in their algorithmic slits.

Because Ultragrams rely on strict adherence to precise geometric constraints in order to produce undistorted images, the above contention that there is a range of

values that prove satisfactory conjures well-founded skepticism. The fact is that this compensation technique does not produce totally distortion-free edge-lit stereograms. The angular match between the algorithmic path and the compensated, refracted ray path which was the basis of this corrective technique is only approximately correct; an unavoidable rounding of values in the computation destroys the elegant precision of the Ultragram and leaves us with a good but not a perfect correction.

If the range of corrective values do not provide an exact correction, then it is probable that each value of separation will result in a different amount of residue distortion. Using the viewband positional shift curve, developed in the last chapter, as a measure of residual distortion we can determine the optimal compensating element to slit master separation. The positional shift curve will also give us a yardstick by which to compare the outcome of this matched-optical-paths technique with last chapter's shift-of-focal-plane technique.

We start by determining the compensating distance to adjust for the viewband at 114 mm along the continuum (since this viewband played the prominent role of the turning point in the shift-of-focal-plane compensation technique). The resultant positional shift graph is shown in Figure 4.9. We observe that the central portion of the curve is very good, with all values below the 0.25 mm figure for viewposition integrity, but that after the compensated zero crossing the positional shift values increase rapidly. By moving the compensation point further out along the abscissa, i.e., by compensating for a viewband further out along the continuum, there will be a smaller domain for this steep rise in positional shift.

We next calculate the distance to compensate for the extreme viewband on the continuum. Here, of course, the extreme viewband is correctly positioned, but as we move towards the center, we quickly reach values that exceed our 0.25 mm criterion. These positional offset values reach a maximum of 0.67 mm before starting to fall off

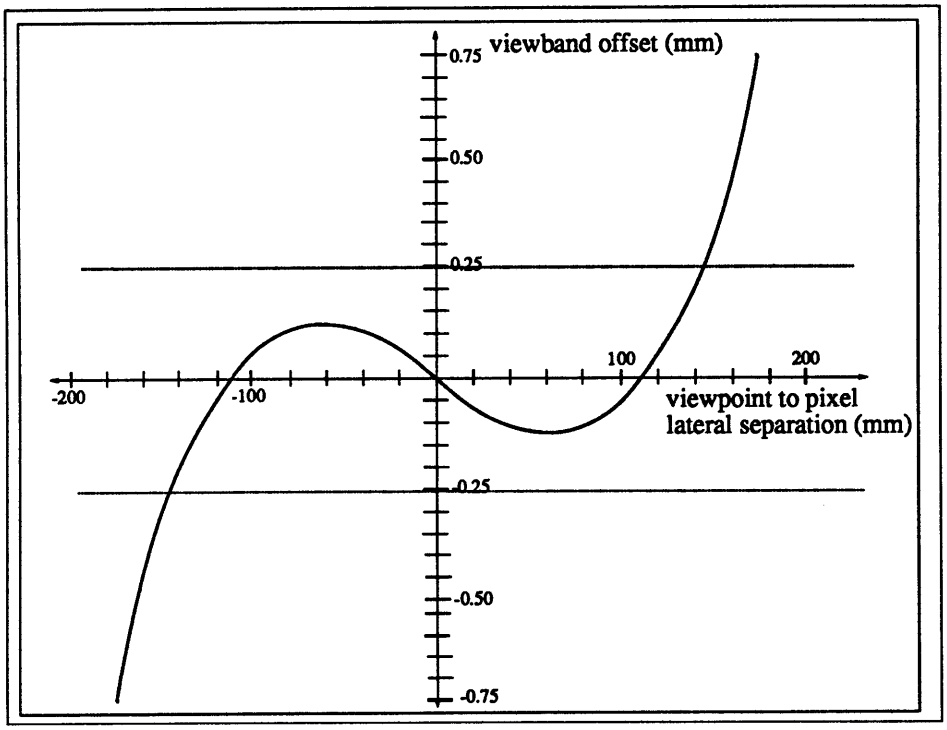

Figure 4.9: The positional shift graph of the continuum when we compensate exactly for the viewband at 114 mm off center.

again.

As we iterate through intermediate values the trade off becomes obvious, i.e., diminished domain of the steep rise experienced at the extreme viewbands in exchange for a greater range and domain of out-of-bound values through the mid-region of the curve. A representative "good" curve is the one for exact compensation of the viewband at 160 mm. The correcting distance for this case is 197.5 mm. This curve is shown in Figure 4.10. It's mid-domain values match with those for the shift-of-focal-plane technique's values; the maximum positional shift in this region is 0.3578 mm (versus 0.3394 mm for the shift-of-focal-plane technique). It is only at the end of the continuum for values above 190 mm that the positional shift values becomes poor. These viewbands will be located at the ends of the Central View Zone, and their pixels will occupy the last few millimeters of image for the far extreme of the Projection Plane, a region that we can expect to have little image detail.

4.7 Conclusion

From the above analysis, we anticipate that an image that is as satisfying in the horizontal extent as that derived from our other shift-of-focal-plane technique, and superior to it from the standpoint of correction the problem of vertical roll can be produced with this matched-optical-paths technique.

An added benefit is reaped from the matched-optical-paths technique. The violation of the distortion-free criterion of this method was a spreading, in the horizontal extent, of the image data in its remap to the View Plane. A similar spreading occurs in the vertical extent. This causes no problem because of the lack of vertical parallax. It is in fact a feature; it results in an increased vertical extent of the view zone

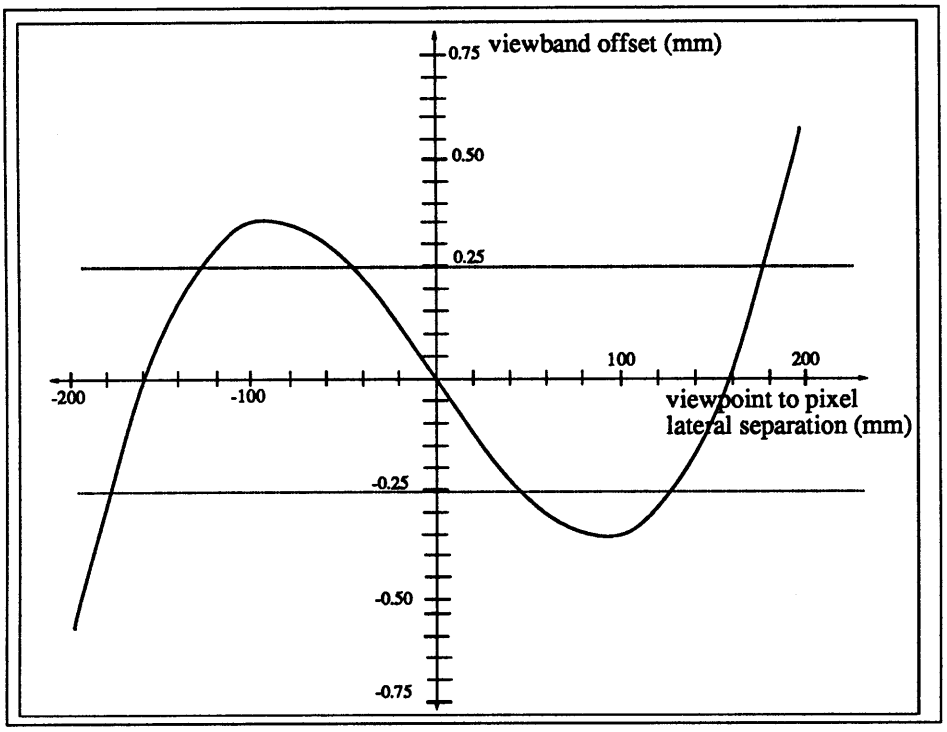

Figure 4.10: A better curve results when we compensate for the viewband at 160 mm.

One the down side, where the shift-of-focal-plane technique, by its simplicity, allowed general Ultragram masters to be transferred into the edge-lit format, the matched-optical-paths technique is far more rigid. The requisite compensating element in the mastering stage restricts the master to the edge-lit format and prevents general Ultragram masters from being used with this technique. Moreover, it prevents masters recorded with this technique to be transferred into other venues.

The analysis and theory of the matched-optical-paths technique await experimental verification.

One final, and brief consideration: our analysis in both this chapter and last have dealt with the image pixels as point values. The pixels in fact have width and the width of the pixel will result in a larger viewband. The 2 mm viewband of our example geometry is in fact a 2.67 mm viewband when the width of the pixel is considered. At viewband boundaries there is a region of intersection where image data for both viewbands' pixel is available (and optically integrated). This overlap provides a relaxing of the 0.25 mm positional shift criterion for viewpoint integrity.

Chapter 5

Immersion Tank Redesign

5.1 Introduction

Because immersion recording had been established as a vital technique of edge-lit holography, the first stage of research involved in the extension of the edge-lit format to holographic stereograms was spent examining the idiosyncrasies of immersion recording. The prototype immersion tank[20] had been fabricated to test whether immersion would improve the images, and whether immersion could be practical. With both answers in the affirmative, our early work with this tank was done with an eye to the design of a permanent production tank. This design was executed and a permanent exposure tank engineered and used for the research reported in this thesis.

The prototype edge-lit immersion tank, diagrammed in Figure 5.1, was a glass tank with a parallelogram geometry. The glass walls and base were joined at the seams by epoxy. The recording plate was held between two point supports attached to the base of the tank and a third point support attached to one-half of the cover

for the tank. After the plate was loaded, the tank was filled with the index-matching

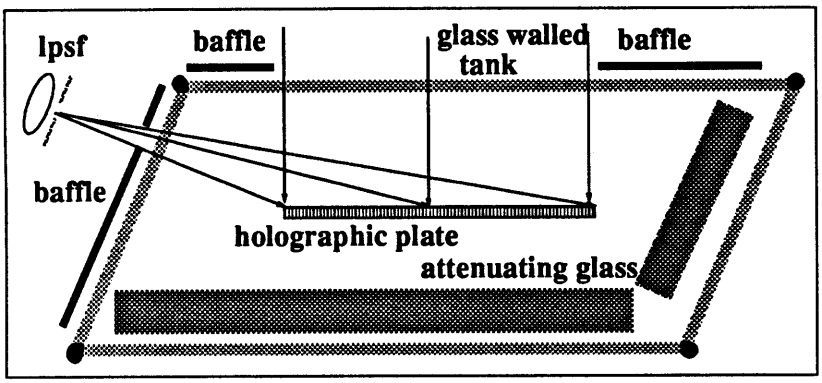

Figure 5.1: Layout of the prototype exposure tank.

liquid, xylene in this case, and the other one-half of the cover was put in place.

5.2 Redesign Considerations

In the design of the new exposure tank, diagrammed in Figure 5.2, changes have been made to the prototype design to increase emulsion efficiency and permit experimental flexibility. The specific changes and their motivations are detailed below.

Geometry: The rhomboidal geometry of the prototype steered waste reference beam light back towards the recording plate.

The trapezoidal shape of the new tank deflects residual light away from the plate. This geometry also increases the number of possible recording configurations from two to four.

Materials: Because the prototype was all glass, all internal surfaces of the tank had significant reflectance.

The new tank is constructed of anodized aluminum, with only the transmission

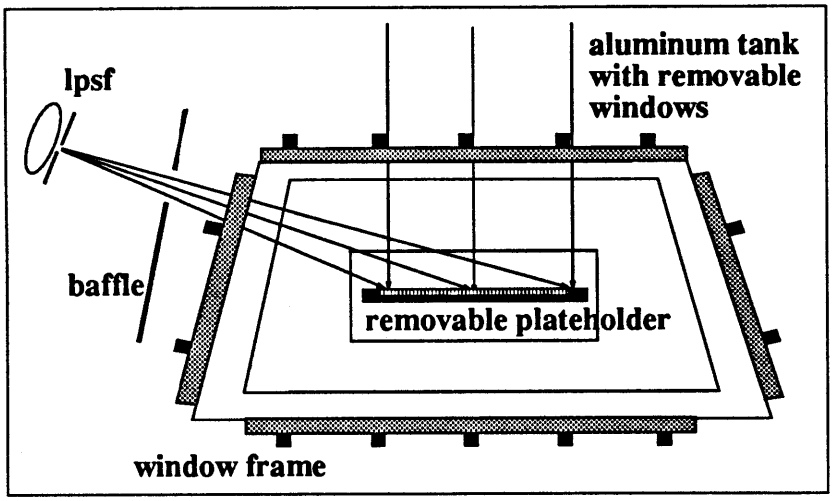

Figure 5.2: The change of geometry and other improvements in the design of the new exposure tank have improved the efficiency of edge-lit holograms.

windows remaining glass. Residual light is steered into corners of anodized aluminum that function as light traps.

Leakage: Xylene, which is used as the index-matching liquid would, over time, cut micro-channels through the epoxy that was used to seal the seams of the prototype tank. Leakage through these micro-channels limited the duration of recording periods.

Because the new tank's frame is composed of aluminum, component pieces can be welded together.

Xylene Contamination: The index-matching liquid quickly became contaminated, resulting from the need to remove and reload the liquid for every shot. This was exacerbated by the need to insert foreign matter – attenuating glass – into the tank prior to exposures. Moreover, the holographer needed to reach into the xylene to remove the exposed plate.

Changes in the geometry and materials of the tank have eliminated the need to

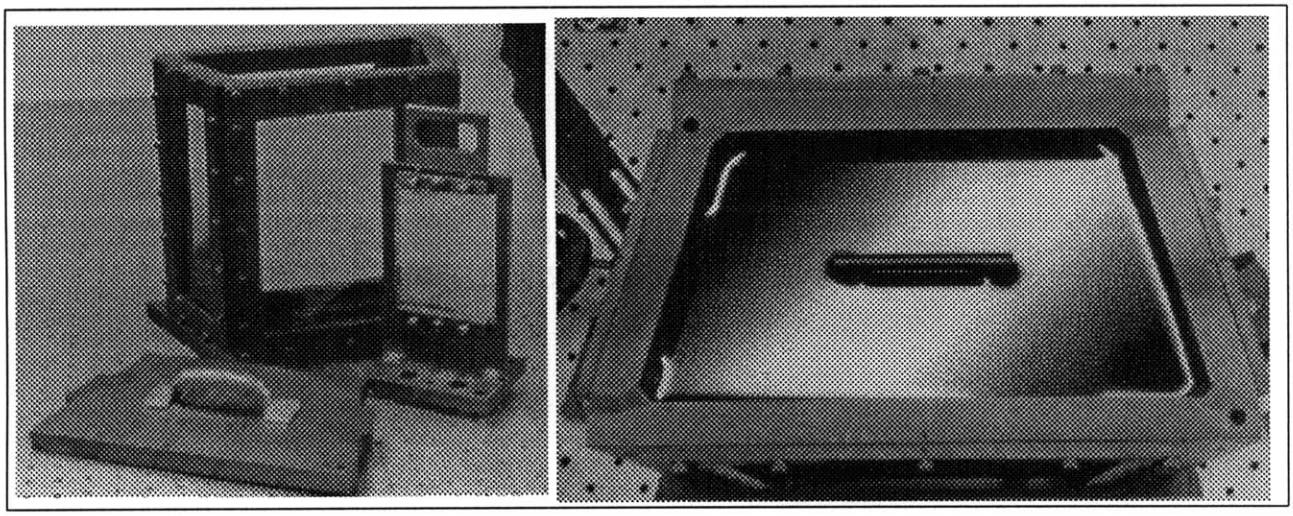

Figure 5.3: Two views of the new immersion tank. On the left, the cover and the plateholder are shown in front of the tank. The right view, from above, shows the handle of the plateholder sitting above the top surface of the xylene.

insert attenuating glasses, eliminating this source of contamination. The incorporation of a removable plateholder eliminates the need to remove and re-add the xylene for each exposure. To spare the holographer, the plateholder can be loaded and removed without putting hands into the xylene. This can be seen in Figure 5.3. The xylene can remain in the tank indefinitely between shots.

Settling Time: Contaminants in the xylene acted as scattering surfaces. After loading the recording plate in the prototype tank, the xylene was reloaded into the tank. This stirred up the contaminants, thereby necessitating long settling times (over an hour).

As stated above, contamination has been greatly reduced. Moreover, the liquid is only mildly agitated by the insertion of the plateholder. We also filter the xylene through fritted glass (50μm) once per month to remove contaminants. The settling time has been reduced to five minutes.

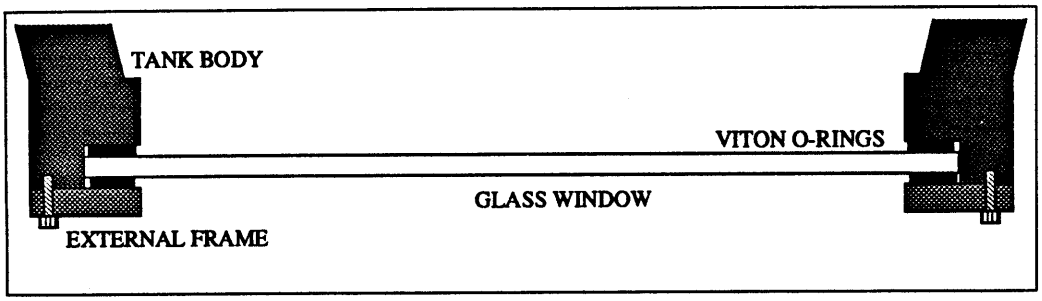

Figure 5.4: The new tank was designed to allow easy replacement of damaged windows. An external frame is used to press the window and o-rings against the body of the tank.

Windows: The monolithic nature of the prototype tank rendered it irreparable. Most significantly, any optical defect in the window portions of the tank was ruinous. The new tank has been designed so that all of the windows are easily replaceable; the framing design is shown in Figure 5.4. O-rings of xylene-resistant viton provide the liquid seal. The size of the windows was chosen such that used hologram plates could be stripped of their emulsion and reused as windows. This provides a cheap source of optical quality windows.

The result of these enhancements in the design of the new exposure tank is that bright, efficient holographic stereograms have been achieved.

Chapter 6

Conclusions

Some final issues involving the research undertaken for this thesis beg mention prior to the conclusion of this thesis. While the research reported here has been highly successful, for the sake of completing the record, it is incumbent to also report the less laudatory aspects of the research. I will attempt to complete the record in this concluding chapter

6.1 Final Thoughts on the Research

The experimental technique used to produce the edge-lit stereogram, i.e., the shift-of-focal-plane-technique, was satisfying not only for the high quality images it is capable of producing, but also for the simplicity with which it can be implemented and the flexibility it brings to a holography facility. This compensation technique allows the use of "off the shelf" masters to be transferred into the edge-lit display format. There is an important limitation to this success, however, that might well be overlooked because of its subtlety.

The master and transfer plates were set parallel to one another during the transfer stage of our experiments. Because of this, the center of our image became the center of symmetry for the refraction. Also, because both our master (300 mm x 300 mm) and transfer (100 mm x 100 mm) plates were square, the geometries of both vertical and horizontal extents were identical. Were the plates not parallel, both the application of the technique and analysis would have been much more difficult. For example, if the plates were mutually angled vertically, then the calculations of viewband continua, a horizontal effect, would have become a function of a viewer's vertical position. Moreover, if our plates were not square then the best compensating distance in the vertical extent would differ from the best compensating distance in the horizontal extent and the holographer would be forced to accept a greater amount of distortion in one dimension or to share the image degradation between both extents.

The problem of asymmetric immersion recording is not academic. With the recording of non-digitized images, i.e., real scenes recorded directly onto 35 mm film, the Ultragram techniques would not be available and traditional stereogram techniques would be used. In these techniques it is unusual to have the master and transfer plates sit parallel to each other.

The matter of square plates is a choice available to the holographer. It does, however, mitigate the flexibility in the use of "off the shelf" masters for transfer into the edge-lit format, if the original master was not constructed in a square format.

Moving beyond acknowledgement of the inherent limitations of our success, there are some aspects of the edge-lit recording technique that are less than optimal. The reference source, for instance, diverges from very near the side wall of the tank, during the transfer stage. The nearer we can place the reference source, the more compact we will be able to make the display apparatus. We used a 65x microscope objective to diverge our beam. It would have been desirable to have gotten even

greater spread in the reference beam than that provided by this objective. The reference beam, like the image beam, is compressed passing through the refractive interface. Because of the proximity of the reference beam to the tank wall and the beam compression experienced on entry into the tank, we get a very uneven intensity distribution and hence density distribution across the lateral extent of our recording. The congestion of apparatus at the edge of the tank is one of several considerations that dissuades the use of a negative lens to boost our spread. Higher power objectives that will give a recording quality beam are rare. It is anticipated that this issue will be resolved as edge-lit recording becomes more widely practiced, and the community develops a toolkit of recording techniques.

In Chapter 5 the issue of xylene contamination was broached. The design of the new immersion tank reduces the rate of contamination, but it does not solve all the problems of working with xylene. While we have managed to reduce the holographers contamination of the xylene, we have not been completely successful in reducing the extent to which the xylene contaminates the holographer. Although the plate can be loaded and removed much more elegantly in the new tank, the exigency of prompt development of the plate, necessitates the removal of the transfer plate from the plate holder while both are still wet with xylenes. While only thin rubber gloves will allow sufficient dexterity for the plate removal, their non-resilience to xylene renders them useless. They are in fact a hazard, because the by-product of their dissolution in the xylene threatens to deface the surface of holographic emulsion. It would be an improvement to replace xylene with a more sympathetic index-matching liquid, but xylene boasts of many admirable properties. An experimental survey of alternate index matching liquids awaits a curious experimenter.

Contamination is not a problem limited to the inside of the tank. Debris on the windows of the tank, especially in the reference beam path has proven a nuisance. The light-scatter from these contaminants is amplified because of the fast divergence

of the reference beam. In one unfortunate case, a large worm in one transfer image was traced to an eyelash on the reference window. Careful attention is necessitated, but some seemingly corrective measures, such as frequently cleaning of the window, tend to attract more particulate matter than they clear. The best solution is a careful cleaning of the entire work space, because the most careful set-up can even be undermined by the dust roused when the curtains are drawn around the table.

Some things go right. There was concern early in the experimentation that stability would be vexing problem. Stability never became an issue. The tank was built such that the insertable plateholder could be fastened to the base of the tank proper with machine screws. This was in fact done in early tests. It was verified experimentally that connecting plateholder to the tank was not necessary, that the kinematic supports on the plateholder provided sufficient stability. The general stability rule-of-thumb became, "if your xylene is stable, your plate is stable".

6.2 Future Research

Edge-lit holography remains a rich experimental vein. The research completed for this thesis, and most all of the research that has been done in the edge-lit format to date, has been broad-stroke experimentation. With the successful extension of the edge-lit format to stereography, it would be appropriate for research to become more compact and address the issue of bringing to the edge-lit display the same degree of technical richness that is available in traditional stereograms.

Beyond the search for a replacement index-matching liquid mentioned above, there are three areas of research that can contribute immensely to edge-lit stereograms specifically, and edge-lit devices in general. The three areas involve research into color control, illumination control, and scaling up the size of edge-lit holograms.

Color issues in stereography have hinged upon intelligent use of the achromatic angle, an angular relationship imposed between the master and transfer plates, that results in the various spectral planes of an image inclining along the same plane in viewer space. The achromatic angle is based upon paraxial approximations, which in the case of the edge-lit stereogram with its large master and small transfer plate, may prove invalid. The disparity in size between the master and transfer plate, the steep intra-emulsion angle of the reference beam, as well as the idiosyncrasies of having two refractive media in our configuration combine to suggest that the orderliness given to color control through use of the achromatic angle may be evasive the case of the edge-lit format. If a different color technique is necessitated the answer may lie in the use of multiple laser lines to record the different colored images. The promise of panchromatic holographic recording materials, if fulfilled, will provide a powerful tool to the color experimentalist.

The illumination of the edge-lit has been relatively unexplored. But, because illumination is the distinguishing characteristic of the format, as experimental issues broaden, illumination will become an area of keen interest. Through the development of clever schemes for the delivery of light, the integration and compactization of the illuminating apparatus that characterizes the edge-lit may be extended to a further minification.

To date, edge-lit holograms have been limited in size to 4″ x 5″. The impact of holograms, like most other display media, can be greatly heighten through an increase of size. Increasing the size of edge-lit holograms may not be a straightforward process. The problems of reference beam spread which are moderately problematic at the current scale, will surely become more pronounced with attempts to scale up the size. In the design of the immersion tank, the front window was designed to be 8″ x 10″, with an eye towards experiments at creating larger holograms. An 8″ x 10″recording plate can be inserted into the frame and reflection edge-lit holograms can be recorded.

These holograms will suffer from artifacts, as did the original edge-lit holograms, but they will provide experimenters with insights into the problems of illumination that will be encountered in trying to scale up the size of edge-lit holograms.

The field is wide open, and the future looks bright for the edge-lit hologram.

6.3 A Summing Up

Since the emergence of holography, there have been periodic claims that the "golden age of holography" was imminent. Yet, like Godot, its imminent arrival goes unrequited. We therefore hesitate to make great claims as to the probable impact of the edge-lit display, but rather offer a modest guess of what might come to pass.

There exist certain venues that would clearly be served by the ability to display images that are three-dimensional. The display of medical images or architectural designs would profit from the increased dimensionality available through holographic stereography. The huge strides made in the ability to generate and display these kinds of images is insufficient in and of itself to pervade these types of venues.

An imaging system, is just that, a system, and chain-like, in that it is as weak as its weakest link. A great impediment to the proliferation of full-dimensional imaging has been the specific technical skill required to merely appropriately display the images; some holographers include illumination devices and instructions with each hologram they sell. Venues, such as those suggested above, require dexterity and flexibility in the display of images. In a medical unit, a simple method of displaying images is necessary. It will be employed by a great many people, doctors, whose expertise does not include holographic illumination. In an architectural environment, transportability of images is requisite, as a designer totes images move from meeting

to meeting. The two requirements enunciated here, simplicity of display and transportability, are both requirements at which the edge-lit excels. So while not wanting to trumpet the imminent arrival of new age, it is with easy modesty that we suggest that the edge-lit display will make a significant contribution to the proliferation of holography. But there is much to be done, developmentally, before the full measure of its potential contribution will be attained.

Bibliography

[1] Dennis Gabor. A New Microscopic Principle. *Nature*, 61:777–778, 1948.

[2] J. T. McCrickerd and N. George. Holographic Stereograms from Sequential Component Photographs. *Applied Physics Letters*, 12:10–12, January 1968.

[3] Domenick J. DeBitetto. Bandwidth Reduction of Hologram Transmission Systems by Elimination of Vertical Parallax. *Applied Physics Letters*, 12–5:176–178, March 1968.

[4] Domenick J. DeBitetto. Holographic Panoramic Stereograms Synthesized from White Light Recordings. *Applied Optics*, 8–8:1740–1741, August 1969.

[5] M. C. King, A. M. Noll, and D. H. Berry. A New Approach to Computer-Generated Holography. *Applied Optics*, 9–2:471–475, February 1970.

[6] Stephen A. Benton. Achromatic Holographic Stereograms. *Journal of the Optical Society of America*, 71–12:1568a, December 1981.

[7] Yuri Denisyuk. *Fundamental of Holography.* Mir Publishers, Moscow, 1978.

[8] P. M. Hariharan. Pseudocolor Images with Volume Reflection Hologram. *Optics Communications*, 35–1:42–44, October 1980.

[9] Julie L. Walker. In Situ Color Control for Reflection Holography. Master's thesis, Massachusetts Institute of Technology, February 1987.

[10] Stephen A. Benton. Alcove Holograms for Computer-Aided Design. In *True Three-Dimensional Imaging Techniques and Display Technologies.* SPIE, 1987.

[11] Mark Holzbach. Three-Dimensional Image Processing for Synthetic Holographic Stereograms. Master's thesis, Massachusetts Institute of Technology, September 1986.

[12] Michael A. Teitel. Anamorphic Raytracing for Synthetic Alcove Holographic Stereograms. Master's thesis, Massachusetts Institute of Technology, September 1986.

[13] Michael Klug. unpublished. Klug has designed an automated system that has produced stereograms of one meter by one meter.

[14] Michael W. Halle. The Generalized Holographic Stereogram. Master's thesis, Massachusetts Institute of Technology, February 1991.

[15] Michael Halle, Stephen Benton, Michael Klug, and John Underkoffler. The Ultragram: A Generalized Holographic Stereogram. In *Practical Holography V.* SPIE, 1991. publication is imminent.

[16] Sabrina M. Birner. Steep Reference Angle Holography: Analysis and Applications. Master's thesis, Massachusetts Institute of Technology, February 1989.

[17] Juris Upatnieks. Compact Holographic Sight. In *Holographic Optics: Design and Applications.* SPIE, 1988.

[18] Stephen A. Benton. Achromatic Images From White-Light Transmission Holograms. *Journal of the Optical Society of America*, 68–10:1441a, October 1978.

[19] Stephen A. Benton, Sabrina M. Birner, and Akira Shirakura. Edge-Lit Rainbow Holograms. In *Practical Holography IV.* SPIE, 1990.

[20] Akira Shirakura. personal communication. Shirakura, Sony Corporation, Electro-Photographic Divison, Tokyo, Japan, undertook the design of the prototype exposure tank. The principles he established have been carried forward in current research and into the present design of the exposure tank.

[21] Stephen A. Benton. Survey of Holographic Stereograms. In *Processing and Display of Three-Dimensional Data.* SPIE, 1983.

[22] Stephen A. Benton. Photographic Holography. In *Optics in Entertainment.* SPIE, 1983.

[23] Stephen A. Benton. Survey of Display Hologram Types. In *Industrial and Commercial Applications of Holography.* SPIE, 1983.